Poiseuille-type flow of a rarefied gas between two parallel plates driven by a uniform external force

Kazuo Aoki,* Shigeru Takata, and Toshiyuki Nakanishi
Department of Aeronautics and Astronautics, Graduate School of Engineering, Kyoto University, Kyoto 606-8501, Japan
(Received 31 August 2001; published 25 January 2002)

A unidirectional flow of a rarefied gas between two parallel plates driven by a uniform external force is investigated on the basis of kinetic theory with special interest in the behavior in the near continuum regime. The Bhatnagar-Gross-Krook (BGK) model of the Boltzmann equation and the diffuse reflection boundary condition are employed as the basic system. First, a systematic asymptotic analysis of the basic system for small Knudsen numbers is carried out, and a system of fluid-dynamic-type equations and their boundary conditions are derived up to the second order in the Knudsen number. Then, an accurate numerical analysis of the original BGK system is performed for a wide range of the Knudsen number by means of a finite-difference method. The behavior of the gas, such as the non-Navier-Stokes effects in the near continuum regime, is clarified on the basis of the fluid-dynamic-type system as well as the numerical solution of the BGK system.

DOI: 10.1103/PhysRevE.65.026315 PACS number(s): 47.45.−n, 51.10.+y, 05.20.Dd, 05.60.−k

I. INTRODUCTION

Let us consider an ideal gas between two parallel infinite plates at rest with a common uniform temperature. When the gas is subject to a uniform external force in the direction parallel to the plates, a steady unidirectional flow of the gas is caused between the plates. If one considers this problem on the basis of the Navier-Stokes equation, it is a simple one-dimensional example.

This classical problem was revisited rather recently in the framework of kinetic theory. Esposito, Lebowitz, and Marra [1] studied its mathematical aspect, that is, they proved the convergence of the solution of the Boltzmann equation to that of the Navier-Stokes equation in the limit where the Knudsen number vanishes (the continuum limit) when the external force is weak. Here, the Knudsen number is the ratio of the mean free path of the gas molecules to the distance between the plates. They also clarified the mathematical structure of the higher-order terms in the Knudsen number. On the other hand, the physical aspect of the problem has been studied by various authors by means of a variety of approximate and numerical methods [2–7]. The main interest of these works is to clarify the phenomena in the near continuum case that cannot be described by the Navier-Stokes equation. One of such phenomena is a bimodal shape of the temperature profile with a slight hollow at the center between the plates. This effect was first pointed out by Malek Mansour, Baras, and Garcia [3] on the basis of a numerical result obtained by the direct simulation Monte Carlo method and of an explicit perturbation solution derived earlier by Tij and Santos [2] using the Bhatnagar-Gross-Krook (BGK) model [8–10]. However, the previous attempts to describe such non-Navier-Stokes effects by macroscopic equations are not satisfactory because no systematic asymptotic analysis has been made for a complete kinetic system containing the boundary condition.

In the present paper, we investigate this problem by means of a systematic asymptotic analysis for small Knudsen numbers as well as a direct numerical analysis on the basis of kinetic theory. To avoid the complexity in the asymptotic analysis and to perform very accurate numerical computation, we utilize the BGK model rather than the Boltzmann equation. But the asymptotic analysis for the latter equation can be carried out in a similar way. In the case where there is no external force, a fluid-dynamic description of rarefied gas flows in the near continuum regime has been established for general geometry by Sone and co-workers [11–19] by means of a systematic asymptotic analysis of the Boltzmann system. In the present paper, we carry out our asymptotic analysis following the asymptotic theory [11–19].

The paper is organized as follows. We first give the formulation of the problem (Sec. II), and then, after setting the appropriate parameter relation that gives the Navier-Stokes equation in the continuum limit, we carry out a systematic asymptotic analysis for small Knudsen numbers to derive a system of fluid-dynamic-type equations and their appropriate boundary conditions (Sec. III). Here, we show that the bimodal shape of the temperature profile mentioned above is attributed to the higher-order correction to the Navier-Stokes solution. An accurate numerical analysis of the original BGK system by a finite-difference method is also carried out for small Knudsen numbers, and the result is compared with that of the asymptotic analysis. In Sec. IV, we carry out the same numerical analysis for a wide range of the Knudsen number and clarify its effect on the physical quantities. A discussion about the result is given in Sec. V, where it is shown that an infinitesimally weak external force can cause a flow of a finite Mach number in the continuum limit.

II. FORMULATION OF THE PROBLEM

A. Problem

Let us consider a rarefied gas between two parallel infinite plates at rest located at $X_1 = L/2$ and $-L/2$ and kept at temperature T_0, where X_i is the rectangular space coordinate system. The gas is subject to a uniform external force in the X_2 direction, i.e., in the direction parallel to the plates. There is no pressure gradient in the X_2 direction. We investigate the steady flow of the gas caused by the external force on the

*Electronic address: kaoki2@ip.media.kyoto-u.ac.jp

basis of kinetic theory for a wide range of the Knudsen number, paying special attention to the behavior for small Knudsen numbers. Our basic assumptions are as follows: (i) The behavior of the gas is described by the BGK model [8–10] of the Boltzmann equation, (ii) the gas molecules are reflected diffusely on the plates.

B. Basic equation

The BGK model of the Boltzmann equation in the present problem is written as [17,20]

$$\xi_1\frac{\partial f}{\partial X_1}+F_2\frac{\partial f}{\partial \xi_2}=A_c\rho(f_e-f), \tag{1}$$

$$f_e=\frac{\rho}{(2\pi RT)^{3/2}}\exp\left(-\frac{(\xi_i-v_i)^2}{2RT}\right), \tag{2}$$

$$\rho=\int f\,d\boldsymbol{\xi}, \tag{3a}$$

$$v_i=\frac{1}{\rho}\int \xi_i f\,d\boldsymbol{\xi}, \tag{3b}$$

$$T=\frac{1}{3R\rho}\int (\xi_i-v_i)^2 f\,d\boldsymbol{\xi}, \tag{3c}$$

where ξ_i is the molecular velocity, $d\boldsymbol{\xi}=d\xi_1 d\xi_2 d\xi_3$, $f(X_1,\xi_i)$ is the velocity distribution function of the gas molecules, $F_i=(0,F_2,0)$ is a uniform external force in the X_2 direction acting on the gas per unit mass, $\rho(X_1)$ is the density of the gas, $v_i(X_1)$ is its flow velocity, $T(X_1)$ is its temperature, R is the gas constant per unit mass, and A_c is a constant ($A_c\rho$ is the collision frequency of a gas molecule, which is independent of the molecular speed). The domain of integration with respect to ξ_i in Eqs. (3a)–(3c) and in Eqs. (7a)–(7c) below is its whole space. The BGK model (1) is consistent with the Boltzmann equation for the (cutoff) Maxwellian molecules (see footnote 21 in Ref. [21]).

The boundary condition on the plates ($X_1=\pm L/2$) is written as follows [17,20]:

$$f=\frac{\rho_w}{(2\pi RT_0)^{3/2}}\exp\left(-\frac{\xi_i^2}{2RT_0}\right)\quad \text{for}\ \ \pm\xi_1>0$$

$$\text{at}\ \ X_1=\mp L/2, \tag{4}$$

$$\rho_w=\mp\left(\frac{2\pi}{RT_0}\right)^{1/2}\int_{\pm\xi_1<0}\xi_1 f(\mp L/2,\xi_i)\,d\boldsymbol{\xi}, \tag{5}$$

where the upper signs correspond to the condition at $X_1=-L/2$, and the lower signs to that at $X_1=L/2$.

Now we assume that f is even in ξ_3, so that $v_3=0$. The analysis below can be performed consistently with this assumption. Further, the integration of Eq. (1) with respect to ξ_i over its whole space leads to $\rho v_1=\text{const}$. Since $\rho v_1=0$ on the boundary because of the diffuse reflection condition [Eqs. (4) and (5)], it turns out that $v_1=0$ identically in the gas. Therefore, it follows from Eqs. (1)–(5) that f is symmetric with respect to the X_2 axis, i.e.,

$$f(X_1,\xi_1,\xi_2,\xi_3)=f(-X_1,-\xi_1,\xi_2,\xi_3). \tag{6}$$

The pressure $p(X_1)$, stress tensor $p_{ij}(X_1)$, and heat-flow vector $q_i(X_1)$ are expressed in terms of f as

$$p=R\rho T=\frac{1}{3}\int (\xi_i-v_i)^2 f\,d\boldsymbol{\xi}, \tag{7a}$$

$$p_{ij}=\int (\xi_i-v_i)(\xi_j-v_j) f\,d\boldsymbol{\xi}, \tag{7b}$$

$$q_i=\frac{1}{2}\int (\xi_i-v_i)(\xi_j-v_j)^2 f\,d\boldsymbol{\xi}. \tag{7c}$$

In addition to $v_1=v_3=0$, the relations $p_{13}(=p_{31})=p_{23}(=p_{32})=0$ and $q_3=0$ follow from the assumption in the preceding paragraph.

C. Dimensionless variables

Let us now introduce the following dimensionless variables:

$$x_i=\frac{X_i}{L},\quad \zeta_i=\frac{\xi_i}{(2RT_0)^{1/2}},\quad \hat f=\frac{(2RT_0)^{3/2}}{\rho_{\rm av}}f,$$

$$\hat\rho=\frac{\rho}{\rho_{\rm av}},\qquad \hat v_i=\frac{v_i}{(2RT_0)^{1/2}},\qquad \hat T=\frac{T}{T_0},$$

$$\hat p=\frac{p}{R\rho_{\rm av}T_0},\qquad \hat p_{ij}=\frac{p_{ij}}{R\rho_{\rm av}T_0}, \tag{8}$$

$$\hat q_i=\frac{q_i}{(\rho_{\rm av}/2)(2RT_0)^{3/2}},$$

where $\rho_{\rm av}$ is the average density of the gas between the plates, and $\hat v_1=\hat v_3=0$ [see the paragraph below Eq. (5)]. Then, the BGK equation, Eqs. (1)–(3c), is written in the following dimensionless form:

$$\zeta_1\frac{\partial \hat f}{\partial x_1}+\hat F\frac{\partial \hat f}{\partial \zeta_2}=\frac{2}{\sqrt{\pi}}\frac{1}{\rm Kn}\hat\rho(\hat f_e-\hat f), \tag{9}$$

$$\hat f_e=\frac{\hat\rho}{(\pi\hat T)^{3/2}}\exp\left(-\frac{\zeta_1^2+(\zeta_2-\hat v_2)^2+\zeta_3^2}{\hat T}\right), \tag{10}$$

$$\hat\rho=\int \hat f\,d\boldsymbol{\zeta}, \tag{11a}$$

$$\hat v_2=\frac{1}{\hat\rho}\int \zeta_2\hat f\,d\boldsymbol{\zeta}, \tag{11b}$$

$$\hat T=\frac{2}{3\hat\rho}\int [\zeta_1^2+(\zeta_2-\hat v_2)^2+\zeta_3^2]\hat f\,d\boldsymbol{\zeta}, \tag{11c}$$

$$\hat F=F_2L(2RT_0)^{-1}, \tag{12a}$$

$$\mathrm{Kn}=2(2RT_0/\pi)^{1/2}(A_c\rho_{\mathrm{av}}L)^{-1}=l_0/L, \tag{12b}$$

where $d\boldsymbol{\zeta}=d\zeta_1 d\zeta_2 d\zeta_3$, Kn is the Knudsen number, l_0 is the mean free path of the gas molecules in the equilibrium state at rest with temperature T_0 and density ρ_{av}, and $\hat{F}$ is the inverse of the Froude number and is a measure of the strength of the external force [l_0 is related to the corresponding viscosity μ_0 and thermal conductivity λ_0 as $\mu_0=(2/5R)\lambda_0=(\sqrt{\pi}/4)\rho_{\mathrm{av}}(2RT_0)^{1/2}l_0$ for the BGK model]. The domain of integration with respect to ζ_i in Eqs. (11a)–(11c) and in what follows is its whole space unless otherwise specified. On the other hand, the dimensionless form of the boundary condition (4) and (5) is given by

$$\hat{f}=\pi^{-3/2}\hat{\rho}_w\exp(-\zeta_i^2) \quad \text{for} \quad \pm\zeta_1>0 \quad \text{at} \quad x_1=\mp 1/2, \tag{13}$$

$$\hat{\rho}_w=\mp 2\pi^{1/2}\int_{\pm\zeta_1<0}\zeta_1\hat{f}(\mp 1/2,\zeta_i)d\boldsymbol{\zeta}, \tag{14}$$

where the upper (or lower) signs correspond to the condition at $x_1=-1/2$ (or $x_1=1/2$). The boundary-value problem, Eqs. (9)–(11c), (13), and (14), is characterized by the two dimensionless parameters $\hat{F}$ and Kn.

The dimensionless forms of Eqs. (7a)–(7c) are given by

$$\hat{p}=\hat{\rho}\hat{T}, \tag{15a}$$

$$\hat{p}_{ij}=2\int(\zeta_i-\hat{v}_i)(\zeta_j-\hat{v}_j)\hat{f}\,d\boldsymbol{\zeta}, \tag{15b}$$

$$\hat{q}_i=\int(\zeta_i-\hat{v}_i)(\zeta_j-\hat{v}_j)^2\hat{f}\,d\boldsymbol{\zeta}. \tag{15c}$$

Note that $\hat{v}_1=\hat{v}_3=0$, $\hat{p}_{13}=\hat{p}_{23}=0$, and $\hat{q}_3=0$.

If we integrate Eq. (9) multiplied by ζ_1, ζ_2, or ζ_j^2 over the whole space of ζ_i and further integrate each result with respect to x_1, then we are led to the following relations:

$$\hat{p}_{11}=\text{const}, \tag{16a}$$

$$\hat{p}_{12}=2\hat{F}\int_0^{x_1}\hat{\rho}\,dx_1, \tag{16b}$$

$$\hat{q}_1=-\int_0^{x_1}\hat{p}_{12}\frac{d\hat{v}_2}{dx_1}dx_1, \tag{16c}$$

where the symmetry of the problem, i.e.,

$$\hat{f}(x_1,\zeta_1,\zeta_2,\zeta_3)=\hat{f}(-x_1,-\zeta_1,\zeta_2,\zeta_3), \tag{17}$$

which leads to $\hat{p}_{12}(0)=\hat{q}_1(0)=0$, has been taken into account.

III. ASYMPTOTIC ANALYSIS FOR SMALL KNUDSEN NUMBERS

In this section we carry out a systematic asymptotic analysis of the boundary-value problem (9)–(11c), (13), and (14) for small Knudsen numbers, following Refs. [11–19], in particular Ref. [12], as a guideline. To begin with, we assume that the parameter $\hat{F}$ for the external force is also small and of the order of the Knudsen number; that is, we put

$$\hat{F}=\alpha\,\mathrm{Kn}=(2/\sqrt{\pi})\alpha\epsilon, \quad \epsilon=(\sqrt{\pi}/2)\mathrm{Kn}\ll 1, \tag{18}$$

where α is a given constant, and ϵ is a small parameter (of the order of Kn) that is mainly used in the following asymptotic analysis. It is known that, in the present problem, this setting of the parameters leads to the (compressible) Navier-Stokes equation with a uniform external-force term in the continuum limit where Kn (or ϵ) vanishes [1].

A. Moderately varying solution

First, putting aside the boundary condition (13) and (14), we look for a moderately varying solution $\hat{f}_H$ to Eqs. (9)–(11c) satisfying $\partial\hat{f}_H/\partial x_1=O(\hat{f}_H)$ in the form of a power series of ϵ:

$$\hat{f}_H=\hat{f}_{H0}+\hat{f}_{H1}\epsilon+\hat{f}_{H2}\epsilon^2+\cdots. \tag{19}$$

This $\hat{f}_H$ is called the Hilbert solution or expansion. Let $\hat{\rho}_H,\hat{T}_H,\hat{v}_{2H},\ldots$ be the macroscopic quantities $\hat{\rho},\hat{T},\hat{v}_2,\ldots$ corresponding to the Hilbert solution. Then, they are also expanded as

$$h_H=h_{H0}+h_{H1}\epsilon+h_{H2}\epsilon^2+\cdots, \tag{20}$$

where h represents $\hat{\rho}$, $\hat{v}_2$, $\hat{T}$, $\hat{p}$, $\hat{p}_{ij}$, or $\hat{q}_i$. The explicit expressions of h_{Hm} in terms of $\hat{f}_{Hm}$ are obtained by substituting $\hat{f}=\hat{f}_H$ and $h=h_H$ in Eqs. (11a)–(11c) and (15a)–(15c) and by equating the coefficients of the same power of ϵ [note that h_{Hm} other than $\hat{\rho}_{Hm}$ also include the lower-order macroscopic quantities ($\hat{\rho}_{Hn}$, $\hat{v}_{2Hn}$, $\hat{T}_{Hn}$, etc. with $n<m$) because the relation between h and $\hat{f}$ in Eqs. (11b), (11c), and (15a)–(15c) is nonlinear]. The explicit expressions of $\hat{\rho}_{Hm}$, $\hat{v}_{2Hm}$, $\hat{T}_{Hm}$, $\hat{p}_{Hm}$, $\hat{p}_{ijHm}$, and $\hat{q}_{iHm}$ for $m=0$, 1, and 2 are given in Appendix A. Now let us denote by $\hat{f}_{eH}$ the local Maxwellian corresponding to the Hilbert solution, i.e., $\hat{f}_e$ with $\hat{\rho}=\hat{\rho}_H$, $\hat{v}_2=\hat{v}_{2H}$, and $\hat{T}=\hat{T}_H$. Then, $\hat{f}_{eH}$ is also expanded as

$$\hat{f}_{eH}=\hat{f}_{eH0}+\hat{f}_{eH1}\epsilon+\hat{f}_{eH2}\epsilon^2+\cdots. \tag{21}$$

The explicit form of the coefficients $\hat{f}_{eHm}$ for $m=0$, 1, and 2 is given in Appendix B. Let $\Psi_r(r=0,\ldots,4)$ stand for the collision invariants, i.e.,

$$\Psi_0=1, \quad \Psi_i=\zeta_i \quad (i=1,2,3), \quad \Psi_4=\zeta_j^2. \tag{22}$$

Since

$$\int\Psi_r(\hat{f}_H-\hat{f}_{eH})d\boldsymbol{\zeta}=0, \tag{23}$$

holds, we have

$$\int \Psi_r(\hat{f}_{Hm}-\hat{f}_{eHm})d\boldsymbol{\zeta}=0 \quad (m=0,1,...). \tag{24}$$

If we substitute the expansions (19)–(21) into Eq. (9) with Eq. (18), we obtain the following expression of $\hat{f}_{Hm}$:

$$\hat{f}_{H0}=\hat{f}_{eH0}, \tag{25}$$

$$\hat{f}_{H1}=\hat{f}_{eH1}-\frac{1}{\hat{\rho}_{H0}}\zeta_1\frac{\partial\hat{f}_{H0}}{\partial x_1}, \tag{26}$$

$$\hat{f}_{Hm}=\hat{f}_{eHm}+\frac{1}{\hat{\rho}_{H0}}\sum_{s=1}^{m-1}\hat{\rho}_{Hs}(\hat{f}_{eHm-s}-\hat{f}_{Hm-s}) - \frac{1}{\hat{\rho}_{H0}}\left(\zeta_1\frac{\partial\hat{f}_{Hm-1}}{\partial x_1}+\frac{2}{\sqrt{\pi}}\alpha\frac{\partial\hat{f}_{Hm-2}}{\partial\zeta_2}\right) \quad (m\geqslant 2). \tag{27}$$

Equation (24) gives the following compatibility conditions for Eqs. (26) and (27):

$$\int \Psi_r\zeta_1\frac{\partial\hat{f}_{H0}}{\partial x_1}d\boldsymbol{\zeta}=0, \tag{28}$$

$$\int \Psi_r\left(\zeta_1\frac{\partial\hat{f}_{Hm-1}}{\partial x_1}+\frac{2}{\sqrt{\pi}}\alpha\frac{\partial\hat{f}_{Hm-2}}{\partial\zeta_2}\right)d\boldsymbol{\zeta}=0 \quad (m\geqslant 2). \tag{29}$$

These conditions are essentially the same as the conservation equations that led to Eqs. (16a)–(16c); but in the procedure of the Hilbert expansion, we put aside the original conservation equations. If we use in Eqs. (28) and (29) the explicit forms of $\hat{f}_{Hn}$ $(n=0,1,...)$ in terms of $\hat{\rho}_{Hs}$, $\hat{v}_{2Hs}$, and $\hat{T}_{Hs}$ $(s\leqslant n)$, which are obtained successively from Eqs. (25)–(27), we obtain a set of ordinary differential equations for the macroscopic quantities $\hat{\rho}_{Hn}$ (or $\hat{p}_{Hn}$), $\hat{v}_{2Hn}$, and $\hat{T}_{Hn}$ (the fluid-dynamic-type equations). More specifically, the equation for $\hat{p}_{H0}$ follows from Eq. (28) with $r=1$ $(\Psi_1=\zeta_1)$ [note that Eq. (28) with $r=2$ and 4 does not add any new equation]; the set for $(\hat{p}_{Hn+1},\hat{v}_{2Hn},\hat{T}_{Hn})(n\geqslant 0)$ follows from Eq. (29) with $m=n+2$ and $r=1$, 2, and 4 $(\Psi_1=\zeta_1,\Psi_2=\zeta_2,\Psi_4=\zeta_j^2)$. Equations (28) and (29) with $r=0$ and 3 $(\Psi_0=1,\Psi_3=\zeta_3)$ are automatically satisfied because we are considering a solution $\hat{f}$ that gives $\hat{v}_1=0$ and is an even function of ζ_3 [see the paragraph after Eq. (5)]. The set of fluid-dynamic-type equations thus obtained is summarized in the following:

$$\frac{d\hat{p}_{H0}}{dx_1}=0, \tag{30}$$

$$\frac{d\hat{p}_{H1}}{dx_1}=0, \tag{31a}$$

$$\frac{d}{dx_1}\left(\hat{T}_{H0}\frac{d\hat{v}_{2H0}}{dx_1}\right)+\frac{4}{\sqrt{\pi}}\alpha\hat{\rho}_{H0}=0, \tag{31b}$$

$$\frac{5}{4}\frac{d}{dx_1}\left(\hat{T}_{H0}\frac{d\hat{T}_{H0}}{dx_1}\right)+\hat{T}_{H0}\left(\frac{d\hat{v}_{2H0}}{dx_1}\right)^2=0, \tag{31c}$$

$$\hat{\rho}_{H0}=\hat{p}_{H0}/\hat{T}_{H0}, \tag{31d}$$

$$\frac{d}{dx_1}\left[\hat{p}_{H2}+\frac{3}{2}\frac{1}{\hat{\rho}_{H0}}\frac{d}{dx_1}\left(\hat{T}_{H0}\frac{d\hat{T}_{H0}}{dx_1}\right)\right]=0, \tag{32a}$$

$$\frac{d}{dx_1}\left(\hat{T}_{H0}\frac{d\hat{v}_{2H1}}{dx_1}+\hat{T}_{H1}\frac{d\hat{v}_{2H0}}{dx_1}\right)+\frac{4}{\sqrt{\pi}}\alpha\hat{\rho}_{H1}=0, \tag{32b}$$

$$\frac{5}{4}\frac{d}{dx_1}\left(\hat{T}_{H0}\frac{d\hat{T}_{H1}}{dx_1}+\hat{T}_{H1}\frac{d\hat{T}_{H0}}{dx_1}\right)+2\hat{T}_{H0}\frac{d\hat{v}_{2H0}}{dx_1}\frac{d\hat{v}_{2H1}}{dx_1} +\hat{T}_{H1}\left(\frac{d\hat{v}_{2H0}}{dx_1}\right)^2=0, \tag{32c}$$

$$\hat{\rho}_{H1}=(\hat{p}_{H1}-\hat{\rho}_{H0}\hat{T}_{H1})/\hat{T}_{H0}, \tag{32d}$$

$$\frac{d}{dx_1}\left\{\hat{p}_{H3}+\frac{3}{2}\frac{1}{\hat{\rho}_{H0}}\left[\frac{d}{dx_1}\left(\hat{T}_{H0}\frac{d\hat{T}_{H1}}{dx_1}+\hat{T}_{H1}\frac{d\hat{T}_{H0}}{dx_1}\right) -\frac{\hat{\rho}_{H1}}{\hat{\rho}_{H0}}\frac{d}{dx_1}\left(\hat{T}_{H0}\frac{d\hat{T}_{H0}}{dx_1}\right)\right]\right\}=0, \tag{33a}$$

$$\frac{d}{dx_1}\left(\hat{T}_{H0}\frac{d\hat{v}_{2H2}}{dx_1}+\hat{T}_{H1}\frac{d\hat{v}_{2H1}}{dx_1}+\hat{T}_{H2}\frac{d\hat{v}_{2H0}}{dx_1}\right) +\frac{56}{\sqrt{\pi}}\frac{\alpha}{\hat{\rho}_{H0}}\left(\frac{d\hat{v}_{2H0}}{dx_1}\right)^2+\frac{4}{\sqrt{\pi}}\alpha\hat{\rho}_{H2}=0, \tag{33b}$$

$$\frac{5}{4}\frac{d}{dx_1}\left(\hat{T}_{H0}\frac{d\hat{T}_{H2}}{dx_1}+\hat{T}_{H1}\frac{d\hat{T}_{H1}}{dx_1}+\hat{T}_{H2}\frac{d\hat{T}_{H0}}{dx_1}\right)+\hat{T}_{H0}\left(\frac{d\hat{v}_{2H1}}{dx_1}\right)^2 +2\hat{T}_{H1}\frac{d\hat{v}_{2H0}}{dx_1}\frac{d\hat{v}_{2H1}}{dx_1}+2\hat{T}_{H0}\frac{d\hat{v}_{2H0}}{dx_1}\frac{d\hat{v}_{2H2}}{dx_1} +\hat{T}_{H2}\left(\frac{d\hat{v}_{2H0}}{dx_1}\right)^2+\frac{72}{25}\frac{\hat{T}_{H0}}{\hat{\rho}_{H0}^2}\left(\frac{d\hat{v}_{2H0}}{dx_1}\right)^4 -\frac{282}{5\sqrt{\pi}}\alpha\frac{\hat{T}_{H0}}{\hat{\rho}_{H0}}\frac{d^2\hat{v}_{2H0}}{dx_1^2}-\frac{256}{\pi}\alpha^2=0, \tag{33c}$$

$$\hat{\rho}_{H2}=(\hat{p}_{H2}-\hat{\rho}_{H0}\hat{T}_{H2}-\hat{\rho}_{H1}\hat{T}_{H1})/\hat{T}_{H0}, \tag{33d}$$

where Eqs. (31d), (32d), and (33d), which give the expressions of $\hat{\rho}_{H0}$, $\hat{\rho}_{H1}$, and $\hat{\rho}_{H2}$, respectively, are the equation of state [see Eqs. (A1d), (A2d), and (A3d)]. Here, some of the equations are not in the form directly corresponding to Eqs. (28) and (29) because they have been simplified with the aid of other equations of the same stage and of the previous

stages. In order to obtain Eqs. (33a)–(33c), we need $\hat{f}_{H3}$ though the explicit form of $\hat{f}_{eH3}$ is not given in Appendix B. In the practical calculations, however, we do not need the explicit form of $\hat{f}_{eHm}$ because the moment $\int \phi(\zeta_i)\hat{f}_{eHm}d\boldsymbol{\zeta}$, where $\phi(\zeta_i)$ is an arbitrary function of ζ_i, can be obtained more easily by calculating $\int \phi(\zeta_i)\hat{f}_{eH}d\boldsymbol{\zeta}$ first and then expanding the result in ϵ.

Substituting the explicit form of $\hat{f}_{Hm}$ $(m=0,1,...)$ into Eqs. (A1e), (A1f), (A2e), (A2f), (A3e), and (A3f), we obtain the expressions of the coefficients $\hat{p}_{ijHm}$ and $\hat{q}_{iHm}$ of the Hilbert expansion of the stress tensor $\hat{p}_{ij}$ and that of the heat-flow vector $\hat{q}_i$ in terms of $\hat{p}_{Hn}$ (or $\hat{\rho}_{Hn}$), $\hat{T}_{Hn}$, and $\hat{v}_{2Hn}$ $(n\leqslant m)$. The results for $m=0$, 1, and 2 are summarized in Appendix C. Corresponding to Eqs. (33a)–(33c), we can also obtain $\hat{p}_{ijH3}$ and $\hat{q}_{iH3}$, but we omit the result because they are rather lengthy.

B. Knudsen-layer correction and slip boundary condition

In the preceding section, we derived the moderately varying solution putting aside the boundary condition, Eqs. (13) and (14). Now we try to construct a solution satisfying the boundary condition. As will be seen, this procedure provides the appropriate boundary conditions for the fluid-dynamic-type equations (30)–(33d).

We first consider the leading-order term $\hat{f}_{H0}$, which is a local Maxwellian given by Eqs. (25) and (B1a). Let us suppose that $\hat{v}_{2H0}$ and $\hat{T}_{H0}$ in $\hat{f}_{H0}$ take the following values on the walls:

$$\hat{v}_{2H0}=0, \quad \hat{T}_{H0}=1, \quad \text{at } x_1=\pm 1/2. \tag{34}$$

Then, it is easily verified that $\hat{f}_{H0}$, with an arbitrary $\hat{\rho}_{H0}$, satisfies the boundary condition, Eqs. (13) and (14). The condition (34) gives the consistent boundary condition for Eqs. (31b)–(31d).

We next consider the first-order term $\hat{f}_{H1}$ given by Eq. (26). By the substitution of Eqs. (25), (B1a), and (B1b) in Eq. (26), it is seen that $\hat{f}_{H1}$ is of the form of $\hat{f}_{eH0}$ multiplied by a polynomial of ζ_i, the highest-order term of which is

$$-\frac{1}{\hat{\rho}_{H0}\hat{T}_{H0}^2}\frac{d\hat{T}_{H0}}{dx_1}\zeta_1\zeta_j^2.$$

In order for $\hat{f}_{H1}$ to fit to the boundary condition, all the coefficients of the polynomial, except the constant term, should vanish on the boundary. However, these constraints lead to the additional conditions $d\hat{v}_{2H0}/dx_1=d\hat{T}_{H0}/dx_1=0$ on the walls. These conditions and Eq. (34) are too many for Eqs. (31b)–(31d) to be solvable. Therefore, $\hat{f}_{H1}$ does not contain the freedom to satisfy the boundary condition. The situation is the same for the higher-order terms $\hat{f}_{Hm}$ $(m\geqslant 2)$. To obtain the solution satisfying the boundary condition, therefore, we need to introduce the so-called Knudsen layers.

Let us seek the solution in the form

$$\hat{f}=\hat{f}_H+\hat{f}_K, \tag{35}$$

with

$$\hat{f}_K=\hat{f}_{K1}\epsilon+\hat{f}_{K2}\epsilon^2+\cdots. \tag{36}$$

Here, $\hat{f}_K$ is the correction to the Hilbert solution $\hat{f}_H$ appreciable only in the thin layers of thickness of the order of ϵ (or of the mean free path in the dimensional X_1 variable) adjacent to the walls (Knudsen layers). The expansion (36) is started from ϵ order because $\hat{f}_{H0}$ could satisfy the boundary condition.

The Knudsen layer at $x_1=-1/2$ and that at $x_1=1/2$ are symmetric with respect to the x_2 axis. To analyze these two Knudsen layers in a unified way, we introduce the following variables:

$$y=x_1+1/2, \quad \eta=y/\epsilon, \quad \zeta_y=\zeta_1, \tag{37}$$

near the wall at $x_1=-1/2$ and

$$y=1/2-x_1, \quad \eta=y/\epsilon, \quad \zeta_y=-\zeta_1, \tag{38}$$

near the wall at $x_1=1/2$. Here, y is the normal coordinate measured from the wall toward the gas, η is the stretched normal coordinate, and ζ_y is the component of ζ_i in the positive y direction. We suppose that the length scale of variation of $\hat{f}_K$ is ϵ, i.e.,

$$\hat{f}_K=\hat{f}_K(\eta,\zeta_y,\zeta_2,\zeta_3), \tag{39}$$

or $\partial\hat{f}_K/\partial\eta=O(\hat{f}_K)$, and that $\hat{f}_K$ vanishes rapidly as $\eta\to\infty$. Corresponding to Eqs. (35) and (36), the macroscopic quantity h, where h represents $\hat{\rho}$, $\hat{v}_2$, $\hat{T}$, $\hat{p}$, $\hat{p}_{ij}$, or $\hat{q}_i$ as before, is expressed as

$$h=h_H+h_K, \tag{40}$$

$$h_K=h_{K1}\epsilon+h_{K2}\epsilon^2+\cdots. \tag{41}$$

The expressions of h_{Km} $(m=1,2,...)$ in terms of $\hat{f}_{Km}$ are obtained as follows. We first substitute Eq. (35) [with Eqs. (19) and (36)] and Eq. (40) [with Eqs. (20) and (41)] into Eqs. (11a)–(11c) and (15a)–(15c) and express the integrals of $\hat{f}_{Hm}$ in terms of h_{Hn} $(n\leqslant m)$ using the relations (A1a)–(A3f). We then expand each h_{Hn} in the Taylor series around the boundary $(y=0)$ as

$$h_{Hn}=(h_{Hn})_B+\left(\frac{dh_{Hn}}{dy}\right)_B\eta\epsilon+\frac{1}{2}\left(\frac{d^2h_{Hn}}{dy^2}\right)_B\eta^2\epsilon^2+\cdots, \tag{42}$$

where $(\,)_B$ indicates the value on the wall (i.e., at $y=0$ or $\eta=0$). If we equate the coefficients of the same power of ϵ, we obtain the desired expression. The explicit form of $\hat{\rho}_{Km}$, $\hat{v}_{2Km}$, $\hat{T}_{Km}$, $\hat{p}_{ijKm}$, and $\hat{q}_{iKm}$ for $m=1$ and 2 is given in Appendix D.

Now we insert Eqs. (35) into Eqs. (9)–(11c) with Eq. (18) and take into consideration the length scale of variation of $\hat{f}_K$

as well as the fact that $\hat{f}_H$ is a solution of Eqs. (9)–(11c). Then, we obtain the following equation for $\hat{f}_K$ [here, the expansions (19) and (36) have not been used yet]:

$$\zeta_y\frac{\partial\hat{f}_K}{\partial\eta}+\frac{2}{\sqrt{\pi}}\alpha\epsilon^2\frac{\partial\hat{f}_K}{\partial\zeta_2}=(\hat{\rho}_H+\hat{\rho}_K)[(\hat{f}_e)_{H+K}-\hat{f}_{eH}-\hat{f}_K]+\hat{\rho}_K(\hat{f}_{eH}-\hat{f}_H), \tag{43}$$

where $(\hat{f}_e)_{H+K}$ stands for $\hat{f}_e$ [Eq. (10)] with $\hat{\rho}=\hat{\rho}_H+\hat{\rho}_K$, $\hat{v}_2=\hat{v}_{2H}+\hat{v}_{2K}$, and $\hat{T}=\hat{T}_H+\hat{T}_K$. If we substitute the expansions (19) (with the explicit form of $\hat{f}_{Hm}$), (20), (36), and (41) and use Eq. (42) as well as the corresponding expansions for the x_1 derivatives of h_{Hn}, then we obtain the sequence of equations for $\hat{f}_{Km}$.

On the other hand, the boundary condition for $\hat{f}_K$ follows from Eqs. (13) and (14) with Eq. (35), that is,

$$(\hat{f}_K)_B=\pi^{-3/2}\hat{\rho}_w\exp(-\zeta^2)-(\hat{f}_H)_B \quad \text{for} \quad \zeta_y>0, \tag{44a}$$

$$\hat{\rho}_w=-2\pi^{1/2}\int_{\zeta_y<0}\zeta_y[(\hat{f}_H)_B+(\hat{f}_K)_B]d\boldsymbol{\zeta}, \tag{44b}$$

on the boundary ($\eta=0$), where

$$\zeta^2=\zeta_y^2+\zeta_2^2+\zeta_3^2, \quad d\boldsymbol{\zeta}=d\zeta_y d\zeta_2 d\zeta_3. \tag{45}$$

Then, substitution of the expansions (19) [with the explicit forms of $\hat{f}_{Hm}$ and the condition (34) for $\hat{f}_{H0}$] and (36) in Eqs. (44a) and (44b) leads to the boundary condition for $\hat{f}_{Km}$.

Now let us put

$$\hat{f}_{Km}=(\hat{\rho}_{H0})_B E\Phi_m \quad (m=1 \text{ and } 2), \qquad E=\pi^{-3/2}\exp(-\zeta^2), \tag{46a}$$

$$y=y'/(\hat{\rho}_{H0})_B, \quad \eta=\eta'/(\hat{\rho}_{H0})_B. \tag{46b}$$

Then, the equations and boundary conditions for $\hat{f}_{K1}$ and $\hat{f}_{K2}$ can be summarized as follows:

$$\zeta_y\frac{\partial\Phi_m}{\partial\eta'}=\mathcal{L}_{\mathrm{BGK}}(\Phi_m)+I_m, \tag{47a}$$

$$\Phi_m=-2\zeta_2(\hat{v}_{2Hm})_B-(\zeta^2-2)(\hat{T}_{Hm})_B-2\sqrt{\pi}\int_{\zeta_y<0}\zeta_y\Phi_m E d\boldsymbol{\zeta}+J_m \quad (\text{for } \zeta_y>0, \text{ at } \eta'=0), \tag{47b}$$

$$\Phi_m\to 0 \quad (\text{rapidly}) \quad (\text{as } \eta'\to\infty), \tag{47c}$$

where $m=1$ and 2, and $\mathcal{L}_{\mathrm{BGK}}$ is the linearized BGK collision operator defined by

$$\mathcal{L}_{\mathrm{BGK}}(\phi)=\int[1+2\zeta_2\overline{\zeta_2}+\tfrac{2}{3}(\zeta^2-\tfrac{3}{2})(\overline{\zeta}^2-\tfrac{3}{2})]\times\phi(\eta',\overline{\zeta_y},\overline{\zeta_2},\overline{\zeta_3})E(\overline{\zeta})d\overline{\boldsymbol{\zeta}}-\phi, \tag{48}$$

with $\overline{\zeta}^2=\overline{\zeta_y}^2+\overline{\zeta_2}^2+\overline{\zeta_3}^2$ and $d\overline{\zeta}=d\overline{\zeta_y}d\overline{\zeta_2}d\overline{\zeta_3}$. The explicit expressions of the terms I_m and J_m are given by

$$I_1=0, \tag{49a}$$

$$\begin{aligned}I_2=&2\zeta_2\left(\zeta^2-\frac{5}{2}\right)\left[(\hat{v}_{2H1})_B+\left(\frac{d\hat{v}_{2H0}}{dy'}\right)_B\eta'+\frac{1}{2}\hat{v}_{2K1}\right]\hat{T}_{K1}\\&+2\zeta_2\left(\zeta^2-\frac{5}{2}\right)\left[(\hat{T}_{H1})_B+\left(\frac{d\hat{T}_{H0}}{dy'}\right)_B\eta'+\frac{1}{2}\hat{T}_{K1}\right]\hat{v}_{2K1}\\&-\frac{4}{3}(\zeta^2-3\zeta_2^2)\left[(\hat{v}_{2H1})_B+\left(\frac{d\hat{v}_{2H0}}{dy'}\right)_B\eta'+\frac{1}{2}\hat{v}_{2K1}\right]\hat{v}_{2K1}\\&+\left(\zeta^4-5\zeta^2+\frac{15}{4}\right)\left[(\hat{T}_{H1})_B+\left(\frac{d\hat{T}_{H0}}{dy'}\right)_B\eta'+\frac{1}{2}\hat{T}_{K1}\right]\hat{T}_{K1}\\&+\mathcal{L}_{\mathrm{BGK}}(\Phi_1)(\hat{\rho}_{H0})_B^{-1}\left[(\hat{\rho}_{H1})_B+\left(\frac{d\hat{\rho}_{H0}}{dy'}\right)_B\eta'+\hat{\rho}_{K1}\right]\\&+\zeta_y\left[\left(\zeta^2-\frac{5}{2}\right)\left(\frac{d\hat{T}_{H0}}{dy'}\right)_B+2\zeta_2\left(\frac{d\hat{v}_{2H0}}{dy'}\right)_B\right]\frac{\hat{\rho}_{K1}}{(\hat{\rho}_{H0})_B},\end{aligned} \tag{49b}$$

$$J_1=2\zeta_y\zeta_2\left(\frac{d\hat{v}_{2H0}}{dy'}\right)_B+\zeta_y\left(\zeta^2-\frac{5}{2}\right)\left(\frac{d\hat{T}_{H0}}{dy'}\right)_B, \tag{50a}$$

$$\begin{aligned}J_2=&-\frac{1}{2}(\zeta^4-5\zeta^2+4)(\hat{T}_{H1})_B^2-(\zeta^2-2)\\&\times(\hat{\rho}_{H0})_B^{-1}(\hat{\rho}_{H1})_B(\hat{T}_{H1})_B-(2\zeta_2^2-1)(\hat{v}_{2H1})_B^2\\&-2\zeta_2(\hat{v}_{2H1})_B\left[\left(\zeta^2-\frac{5}{2}\right)(\hat{T}_{H1})_B+\frac{(\hat{\rho}_{H1})_B}{(\hat{\rho}_{H0})_B}\right]+\zeta_y\left\{\left(\zeta^2\right.\right.\\&\left.-\frac{5}{2}\right)\left(\frac{d\hat{T}_{H1}}{dy'}\right)_B+2\zeta_2\left(\frac{d\hat{v}_{2H1}}{dy'}\right)_B+\left[\left(\zeta^4-6\zeta^2+\frac{25}{4}\right)\right.\\&\times(\hat{T}_{H1})_B+2\zeta_2\left(\zeta^2-\frac{7}{2}\right)(\hat{v}_{2H1})_B\left]\left(\frac{d\hat{T}_{H0}}{dy'}\right)_B+\left[2\zeta_2\left(\zeta^2\right.\right.\right.\\&\left.\left.\left.-\frac{5}{2}\right)(\hat{T}_{H1})_B+2(2\zeta_2^2-1)(\hat{v}_{2H1})_B\right]\left(\frac{d\hat{v}_{2H0}}{dy'}\right)_B\right\}\\&-\zeta_y^2\left[\left(\zeta^4-7\zeta^2+\frac{35}{4}\right)\left(\frac{d\hat{T}_{H0}}{dy'}\right)_B^2+4\left(\zeta_2^2-\frac{1}{5}\zeta^2\right)\right.\\&\left.\times\left(\frac{d\hat{v}_{2H0}}{dy'}\right)_B^2+4\zeta_2\left(\zeta^2-\frac{7}{2}\right)\left(\frac{d\hat{T}_{H0}}{dy'}\right)_B\left(\frac{d\hat{v}_{2H0}}{dy'}\right)_B\right]\end{aligned}$$

$$-\frac{1}{4}\left(\frac{d\hat{T}_{H0}}{dy'}\right)_B^2-\frac{2}{5}\left(\frac{d\hat{v}_{2H0}}{dy'}\right)_B^2+\frac{4}{\sqrt{\pi}}\frac{\alpha}{(\hat{\rho}_{H0})_B}\zeta_2(2\zeta_y^2-1). \tag{50b}$$

The problem (47a)–(47c) for Φ_m is a one-dimensional boundary-value problem (half-space problem) of the linearized BGK equation. This problem with general I_m and J_m [i.e., I_m and J_m that are not restricted to the forms of Eqs. (49a)–(50b)] has the following property. For given $I_m(\eta',\zeta_y,\zeta_2,\zeta_3)$ that vanishes rapidly as $\eta'\to\infty$ and $J_m(\zeta_y,\zeta_2,\zeta_3)$, the solution Φ_m is determined together with the constants $(\hat{v}_{2Hm})_B$ and $(\hat{T}_{Hm})_B$ contained in the boundary condition (47b). The boundary values $(\hat{v}_{2H1})_B$ and $(\hat{T}_{H1})_B$ thus determined give the boundary condition for the fluid-dynamic-type equations (32b)–(32d), and those $(\hat{v}_{2H2})_B$ and $(\hat{T}_{H2})_B$ give the boundary condition for Eqs. (33b)–(33d).

The property of the problem (47a)–(47c) described in the preceding paragraph is also true for the linearized Boltzmann equation, i.e., Eq. (47a) with $\mathcal{L}_{\mathrm{BGK}}$ replaced by the linearized Boltzmann collision operator. Grad [22] conjectured the existence and uniqueness of the solution and the constants in the boundary condition $[(\hat{v}_{Hm})_B$ and $(\hat{T}_{Hm})_B]$. Grad's conjectured theorem was later proved by Bardos, Caflisch, and Nicolaenko [23] for hard-sphere molecules and by Cercignani [24] and by Golse and Poupaud [25] for more general molecular models. The reader is referred to Refs. [16], [18], [19] for further discussions about the theorem.

In the actual calculation, we can obtain the solution to Eqs. (47a)–(47c) in the form

$$\Phi_m=\Phi_m^o+\Phi_m^e, \tag{51}$$

where Φ_m^o is odd in ζ_2, and Φ_m^e is even in ζ_2. In view of the explicit form of I_m and J_m, we can put

$$\begin{bmatrix}\Phi_1^o\\(\hat{v}_{2H1})_B\end{bmatrix}=\begin{bmatrix}\psi_{1a}\\\beta_{1a}\end{bmatrix}\left(\frac{d\hat{v}_{2H0}}{dy'}\right)_B, \tag{52a}$$

$$\begin{bmatrix}\Phi_1^e\\(\hat{T}_{H1})_B\end{bmatrix}=\begin{bmatrix}\tilde{\psi}_{1a}\\\tilde{\beta}_{1a}\end{bmatrix}\left(\frac{d\hat{T}_{H0}}{dy'}\right)_B, \tag{52b}$$

$$\begin{bmatrix}\Phi_2^o\\(\hat{v}_{2H2})_B\end{bmatrix}=\begin{bmatrix}\psi_{2a}\\\beta_{2a}\end{bmatrix}\left(\frac{d\hat{v}_{2H1}}{dy'}\right)_B+\begin{bmatrix}\psi_{2b}\\\beta_{2b}\end{bmatrix}\frac{(\hat{\rho}_{H1})_B}{(\hat{\rho}_{H0})_B}\left(\frac{d\hat{v}_{2H0}}{dy'}\right)_B+\begin{bmatrix}\psi_{2c}\\\beta_{2c}\end{bmatrix}\left(\frac{d\hat{v}_{2H0}}{dy'}\right)_B\left(\frac{d\hat{T}_{H0}}{dy'}\right)_B+\begin{bmatrix}\psi_{2d}\\\beta_{2d}\end{bmatrix}\frac{\alpha}{(\hat{\rho}_{H0})_B}, \tag{53a}$$

$$\begin{bmatrix}\Phi_2^e\\(\hat{T}_{H2})_B\end{bmatrix}=\begin{bmatrix}\tilde{\psi}_{2a}\\\tilde{\beta}_{2a}\end{bmatrix}\left(\frac{d\hat{T}_{H1}}{dy'}\right)_B+\begin{bmatrix}\tilde{\psi}_{2b}\\\tilde{\beta}_{2b}\end{bmatrix}\frac{(\hat{\rho}_{H1})_B}{(\hat{\rho}_{H0})_B}\left(\frac{d\hat{T}_{H0}}{dy'}\right)_B+\begin{bmatrix}\tilde{\psi}_{2c}\\\tilde{\beta}_{2c}\end{bmatrix}\left(\frac{d\hat{T}_{H0}}{dy'}\right)_B^2+\begin{bmatrix}\tilde{\psi}_{2d}\\\tilde{\beta}_{2d}\end{bmatrix}\left(\frac{d\hat{v}_{2H0}}{dy'}\right)_B^2, \tag{53b}$$

where $\psi_{1a},\psi_{2a},\ldots,\psi_{2d}$ are odd in ζ_2, $\tilde{\psi}_{1a},\tilde{\psi}_{2a},\ldots,\tilde{\psi}_{2d}$ are even in ζ_2, and $\beta_{1a},\beta_{2a},\ldots,\beta_{2d}$ and $\tilde{\beta}_{1a},\tilde{\beta}_{2a},\ldots,\tilde{\beta}_{2d}$ are constants. In deriving the form of Eqs. (53a) and (53b), we have used the form (52a) and (52b) in I_2 and J_2. Then, we analyze each decomposed problem to determine (ψ_{1a},β_{1a}), $(\tilde{\psi}_{1a},\tilde{\beta}_{1a})$, (ψ_{2a},β_{2a}), $(\tilde{\psi}_{2a},\tilde{\beta}_{2a})$, etc. numerically by a finite-difference method. Once Φ_1 and Φ_2 are determined, we can calculate the Knudsen-layer part of the macroscopic variables by using Eqs. (D1a)–(D2i). Here, we summarize the boundary conditions for Eqs. (32b)–(32d) and (33b)–(33d) and the Knudsen-layer parts of the flow velocity, density, and temperature thus obtained, using the original coordinate y rather than y'.

The boundary condition for Eqs. (32b)–(32d) on the walls $(y=0)$ is [note Eqs. (37) and (38) for the relation between y and x_1]

$$(\hat{v}_{2H1})_B=\beta_{1a}\frac{1}{(\hat{\rho}_{H0})_B}\left(\frac{d\hat{v}_{2H0}}{dy}\right)_B, \tag{54a}$$

$$(\hat{T}_{H1})_B=\tilde{\beta}_{1a}\frac{1}{(\hat{\rho}_{H0})_B}\left(\frac{d\hat{T}_{H0}}{dy}\right)_B, \tag{54b}$$

$$\beta_{1a}=1.016\,19,\quad \tilde{\beta}_{1a}=1.302\,72. \tag{54c}$$

The boundary condition for Eqs. (33b)–(33d) on the walls is

$$(\hat{v}_{2H2})_B=\beta_{2a}\frac{1}{(\hat{\rho}_{H0})_B}\left(\frac{d\hat{v}_{2H1}}{dy}\right)_B+\beta_{2b}\frac{(\hat{\rho}_{H1})_B}{(\hat{\rho}_{H0})_B^2}\left(\frac{d\hat{v}_{2H0}}{dy}\right)_B+\beta_{2c}\frac{1}{(\hat{\rho}_{H0})_B^2}\left(\frac{d\hat{v}_{2H0}}{dy}\right)_B\left(\frac{d\hat{T}_{H0}}{dy}\right)_B+\beta_{2d}\frac{\alpha}{(\hat{\rho}_{H0})_B}, \tag{55a}$$

$$(\hat{T}_{H2})_B=\tilde{\beta}_{2a}\frac{1}{(\hat{\rho}_{H0})_B}\left(\frac{d\hat{T}_{H1}}{dy}\right)_B+\tilde{\beta}_{2b}\frac{(\hat{\rho}_{H1})_B}{(\hat{\rho}_{H0})_B^2}\left(\frac{d\hat{T}_{H0}}{dy}\right)_B+\tilde{\beta}_{2c}\frac{1}{(\hat{\rho}_{H0})_B^2}\left(\frac{d\hat{T}_{H0}}{dy}\right)_B^2+\tilde{\beta}_{2d}\frac{1}{(\hat{\rho}_{H0})_B^2}\left(\frac{d\hat{v}_{2H0}}{dy}\right)_B^2, \tag{55b}$$

$$\beta_{2a}=\beta_{1a},\quad \beta_{2b}=-1.016\,19,\quad \beta_{2c}=-0.831\,03,\quad \beta_{2d}=1.729\,42,$$

$$\tilde{\beta}_{2a}=\tilde{\beta}_{1a},\quad \tilde{\beta}_{2b}=-1.302\,71,\quad \tilde{\beta}_{2c}=-1.393\,17,\quad \tilde{\beta}_{2d}=1.161\,72. \tag{55c}$$

The Knudsen-layer parts of the flow velocity, density, and temperature are given by

$$\hat{v}_{2K1}=Y_a(\eta')\frac{1}{(\hat{\rho}_{H0})_B}\left(\frac{d\hat{v}_{2H0}}{dy}\right)_B, \tag{56a}$$

TABLE I. Knudsen-layer functions.

η'	Ω_a	$-\Theta_a$	$-Y_a$	$-\Omega_b$	Θ_b	Y_b	$-\Omega_c$	Θ_c	Y_c	Ω_d	$-\Theta_d$	$-Y_d$
0.0	0.347 72	0.449 21	0.309 09	−0.000 02	0.449 19	0.309 08	1.305 35	0.956 99	0.527 59	0.092 25	0.449 00	1.236 20
0.05	0.291 77	0.385 21	0.257 27	0.036 77	0.428 83	0.291 97	1.277 15	0.935 87	0.520 43	0.064 83	0.405 95	1.085 91
0.1	0.261 21	0.348 42	0.228 28	0.051 74	0.411 60	0.277 57	1.256 59	0.913 30	0.508 79	0.049 99	0.376 16	0.992 11
0.2	0.219 87	0.297 04	0.188 78	0.067 32	0.382 15	0.253 19	1.218 36	0.869 35	0.483 98	0.030 73	0.330 65	0.854 79
0.3	0.190 96	0.260 06	0.161 14	0.075 00	0.357 02	0.232 69	1.181 14	0.827 52	0.459 38	0.018 22	0.295 56	0.752 07
0.4	0.168 77	0.231 14	0.140 03	0.078 97	0.334 93	0.214 92	1.144 38	0.787 79	0.435 66	0.009 41	0.266 90	0.669 78
0.5	0.150 91	0.207 52	0.123 16	0.080 86	0.315 15	0.199 23	1.108 07	0.750 06	0.413 02	0.002 97	0.242 77	0.601 46
0.6	0.136 10	0.187 70	0.109 29	0.081 46	0.297 24	0.185 23	1.072 30	0.714 22	0.391 50	−0.001 82	0.222 04	0.543 45
0.7	0.123 55	0.170 75	0.097 64	0.081 23	0.280 88	0.172 62	1.037 15	0.680 15	0.371 09	−0.005 42	0.203 98	0.493 44
0.8	0.112 75	0.156 06	0.087 72	0.080 43	0.265 84	0.161 18	1.002 72	0.647 76	0.351 75	−0.008 12	0.188 08	0.449 80
0.9	0.103 34	0.143 18	0.079 18	0.079 25	0.251 95	0.150 76	0.969 05	0.616 96	0.333 45	−0.010 15	0.173 95	0.411 39
1.0	0.095 06	0.131 80	0.071 74	0.077 79	0.239 07	0.141 22	0.936 20	0.587 65	0.316 12	−0.011 65	0.161 32	0.377 32
1.2	0.081 17	0.112 57	0.059 47	0.074 40	0.215 89	0.124 39	0.873 04	0.533 20	0.284 20	−0.013 49	0.139 67	0.319 68
1.4	0.069 98	0.096 99	0.049 82	0.070 67	0.195 60	0.110 02	0.813 36	0.483 84	0.255 62	−0.014 27	0.121 83	0.272 95
1.6	0.060 79	0.084 15	0.042 08	0.066 83	0.177 69	0.097 65	0.757 19	0.439 06	0.230 02	−0.014 38	0.106 92	0.234 53
1.8	0.053 14	0.073 43	0.035 79	0.063 01	0.161 79	0.086 93	0.704 46	0.398 41	0.207 07	−0.014 06	0.094 32	0.202 58
2.0	0.046 70	0.064 39	0.030 62	0.059 29	0.147 60	0.077 59	0.655 06	0.361 50	0.186 50	−0.013 47	0.083 56	0.175 77
2.5	0.034 41	0.047 16	0.021 17	0.050 64	0.118 15	0.058 92	0.545 26	0.283 31	0.143 81	−0.011 46	0.062 70	0.125 24
3.0	0.025 87	0.035 19	0.014 97	0.043 06	0.095 33	0.045 23	0.453 04	0.221 69	0.111 14	−0.009 30	0.047 88	0.090 86
3.5	0.019 73	0.026 65	0.010 77	0.036 54	0.077 39	0.035 01	0.375 94	0.173 09	0.086 05	−0.007 33	0.037 06	0.066 86
4.0	0.015 23	0.020 41	0.007 87	0.030 97	0.063 13	0.027 28	0.311 68	0.134 74	0.066 74	−0.005 67	0.028 99	0.049 76
5.0	0.009 31	0.012 30	0.004 33	0.022 22	0.042 52	0.016 85	0.213 81	0.080 64	0.040 29	−0.003 24	0.018 18	0.028 32
6.0	0.005 84	0.007 62	0.002 47	0.015 95	0.029 00	0.010 59	0.146 40	0.047 10	0.024 41	−0.001 74	0.011 69	0.016 58
8.0	0.002 43	0.003 10	0.000 86	0.008 25	0.013 86	0.004 35	0.068 34	0.013 91	0.009 00	−0.000 38	0.005 09	0.006 05
10.0	0.001 07	0.001 33	0.000 32	0.004 29	0.006 81	0.001 86	0.031 71	0.002 11	0.003 30	0.000 01	0.002 32	0.002 34

$$\begin{bmatrix} \hat{\rho}_{K1}/(\hat{\rho}_{H0})_B \\ \hat{T}_{K1} \end{bmatrix} = \begin{bmatrix} \Omega_a(\eta') \\ \Theta_a(\eta') \end{bmatrix} \frac{1}{(\hat{\rho}_{H0})_B} \left(\frac{d\hat{T}_{H0}}{dy} \right)_B, \quad (56b)$$

$$\hat{v}_{2K2} = Y_a(\eta') \frac{1}{(\hat{\rho}_{H0})_B} \left(\frac{d\hat{v}_{2H1}}{dy} \right)_B + Y_b(\eta') \frac{(\hat{\rho}_{H1})_B}{(\hat{\rho}_{H0})_B^2} \left(\frac{d\hat{v}_{2H0}}{dy} \right)_B + Y_c(\eta') \frac{1}{(\hat{\rho}_{H0})_B^2} \left(\frac{d\hat{v}_{2H0}}{dy} \right)_B \left(\frac{d\hat{T}_{H0}}{dy} \right)_B + Y_d(\eta') \frac{\alpha}{(\hat{\rho}_{H0})_B}, \quad (57a)$$

$$\begin{bmatrix} \hat{\rho}_{K2}/(\hat{\rho}_{H0})_B \\ \hat{T}_{K2} \end{bmatrix} = \begin{bmatrix} \Omega_a(\eta') \\ \Theta_a(\eta') \end{bmatrix} \frac{1}{(\hat{\rho}_{H0})_B} \left(\frac{d\hat{T}_{H1}}{dy} \right)_B + \begin{bmatrix} \Omega_b(\eta') \\ \Theta_b(\eta') \end{bmatrix} \frac{(\hat{\rho}_{H1})_B}{(\hat{\rho}_{H0})_B^2} \left(\frac{d\hat{T}_{H0}}{dy} \right)_B + \begin{bmatrix} \Omega_c(\eta') \\ \Theta_c(\eta') \end{bmatrix} \frac{1}{(\hat{\rho}_{H0})_B^2} \left(\frac{d\hat{T}_{H0}}{dy} \right)_B^2 + \begin{bmatrix} \Omega_d(\eta') \\ \Theta_d(\eta') \end{bmatrix} \frac{1}{(\hat{\rho}_{H0})_B^2} \left(\frac{d\hat{v}_{2H0}}{dy} \right)_B^2, \quad (57b)$$

where η' [Eq. (46b)] rather than η is used as the variable of the functions Y_a, Ω_a, Θ_a, etc. These are universal functions of η' only, which we call Knudsen-layer functions. These functions are shown in Table I. The relations $\beta_{1a} = -\beta_{2b}$ and $\tilde{\beta}_{1a} = -\tilde{\beta}_{2b}$ are likely to hold; the differences would be attributed to the numerical error. But the corresponding Knudsen-layer functions are different.

Some of the slip coefficients, Eqs. (54c) and (55c), and the Knudsen-layer functions occurring in Eqs. (56a)–(57b) are those obtained earlier [11,12,26–29] (see also Refs. [17–19]). For instance,

$$[\beta_{1a}, Y_a(x)] = [\kappa_1, \Delta_1(x)] \text{ (Ref.[12])} = [-k_0, -Y_0(x)] \text{ (Refs. [17–19] and [29])}, \quad (58a)$$

$$[\tilde{\beta}_a, \Omega_a(x), \Theta_a(x)] = [\alpha_1, \Omega_1(x), \Theta_1(x)] \text{ (Ref.[12])} = [d_1, \Omega_1(x), \Theta_1(x)] \text{ (Refs. [17–19] and [29])}, \quad (58b)$$

where the variable x is commonly used as the independent variable of the Knudsen-layer functions. In these earlier works, the Knudsen-layer problems, represented by the form of Eqs. (47a)–(47c), are first transformed into the integral equations for the Knudsen-layer parts of the macroscopic

quantities $\hat{v}_{2Km}$, $\hat{\rho}_{Km}$, and $\hat{T}_{Km}$. This transformation can be made by writing $\mathcal{L}_{\mathrm{BGK}}(\Phi_m)$ in terms of $\hat{v}_{2Km}$, $\hat{\rho}_{Km}$, and $\hat{T}_{Km}$ [see Eqs. (D1a)–(D1c) and (D2a)–(D2c)], by integrating Eq. (47a) formally under Eqs. (47b) and (47c), and then by substituting the resulting Φ_m into the definition of $\hat{v}_{2Km}$, $\hat{\rho}_{Km}$, and $\hat{T}_{Km}$. The integral equations are then solved by a moment method devised by Sone [26,27] and improved by Sone and Onishi [28,29]. However, since the direct numerical solution of Eqs. (47a)–(47c) by a finite-difference method is rather easy nowadays, we made use of this method here (see the last paragraph in Sec. IV A). Incidentally, (β_{1a}, Y_a) and $(\tilde{\beta}_{1a}, \Omega_a, \Theta_a)$ are obtained also for a hard-sphere gas by means of an accurate finite-difference method for the linearized Boltzmann equation: $[\beta_{1a}, Y_a(x)] = [\beta_A, S(x)]$ in Ref. [30] and $[\tilde{\beta}_{1a}, \Omega_a(x), \Theta_a(x)] = [\beta, \Omega(x), \Theta(x)]$ in Ref. [31].

C. Flow properties at small Knudsen numbers

In the preceding sections, we have derived the fluid-dynamic-type equations (30)–(33d), their boundary conditions (34) and (54a)–(55c), and the Knudsen-layer corrections (56a)–(57b) for the macroscopic quantities. In this section, we discuss the flow properties for small Knudsen numbers on the basis of these results.

We first compare the fluid-dynamic-type equations (30)–(33d) with the (compressible) Navier-Stokes equations, more precisely, the equations obtained from the Navier-Stokes equations by means of the expansion corresponding to Eq. (19) [note that the viscosity $\mu = (T/T_0)\mu_0$ and the thermal conductivity $\lambda = (T/T_0)\lambda_0$, which correspond to the BGK model (see the first paragraph in Sec. II C for μ_0 and λ_0), should be used together with the relation (18)]. Equation (30) is the degenerated Euler equation, and Eqs. (31a)–(31d) are the same as the Navier-Stokes equations. The next-order equations (32b)–(32d) are also the same as the corresponding Navier-Stokes equations, whereas the second term in the square brackets in Eq. (32a) is not contained in the Navier-Stokes equations. In Eqs. (33a)–(33c), many non-Navier-Stokes terms appear, i.e., the terms other than the first term in the curly brackets of Eq. (33a), the term with the coefficient $56/\sqrt{\pi}$ in Eq. (33b), and the terms with the coefficients $72/25$, $-282/5\sqrt{\pi}$, and $-256/\pi$ in Eq. (33c).

In Figs. 1–3, we show the solutions $\hat{\rho}_{Hm}$, $\hat{v}_{2Hm}$, and $\hat{T}_{Hm}$ ($m=0$, 1, and 2) of the fluid-dynamic systems for several values of α [cf. Eq. (18)]. More specifically, the solution to Eqs. (30) and (31b)–(31d) with the nonslip condition (34) is shown in Fig. 1, that to Eqs. (31a) and (32b)–(32d) with the slip condition (54a)–(54c) in Fig. 2, and that to Eqs. (32a) and (33b)–(33d) with the slip condition (55a)–(55c) in Fig. 3. Since these solutions are symmetric with respect to the x_2 axis, the right half ($0 \leqslant x_1 \leqslant 0.5$) is shown in the figures. The results shown in the figures are the numerical solutions. Here, the density is normalized as follows. If we use Eqs. (40), (20), and (41) with $h = \hat{\rho}$ in the definition of ρ_{av}, i.e.,

$$\rho_{\mathrm{av}} = \frac{1}{L}\int_{-L/2}^{L/2} \rho dX_1 = 2\rho_{\mathrm{av}} \int_0^{1/2} \hat{\rho} dx_1, \tag{59}$$

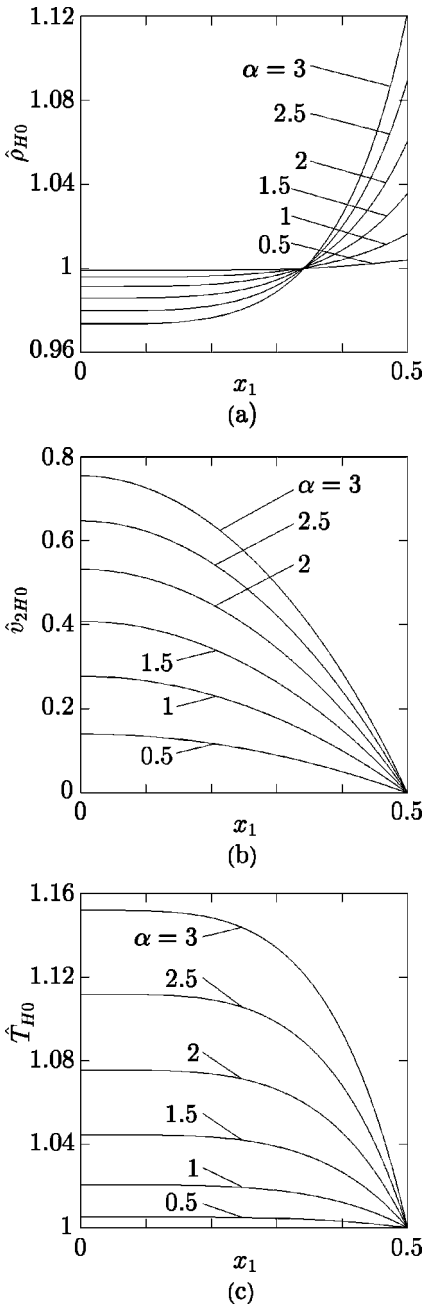

FIG. 1. The solution $\hat{\rho}_{H0}$, $\hat{v}_{2H0}$, and $\hat{T}_{H0}$ for various α. (a) $\hat{\rho}_{H0}$, (b) $\hat{v}_{2H0}$, (c) $\hat{T}_{H0}$.

and recall that $\hat{\rho}_K$ is the function of η, then we have

$$\int_0^{1/2} \hat{\rho}_{H0} dx_1 = \frac{1}{2}, \tag{60a}$$

$$\int_0^{1/2} \hat{\rho}_{H1} dx_1 = 0, \tag{60b}$$

$$\int_0^{1/2} \hat{\rho}_{H2} dx_1 = -\int_0^{\infty} \hat{\rho}_{K1} d\eta. \tag{60c}$$

These are the normalization conditions.

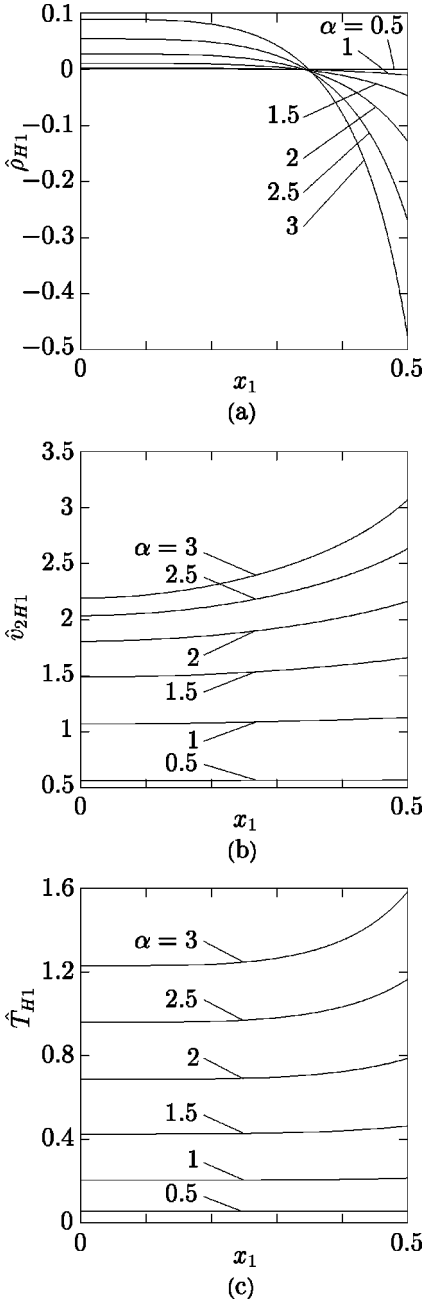

FIG. 2. The solution $\hat{\rho}_{H1}$, $\hat{v}_{2H1}$, and $\hat{T}_{H1}$ for various α. (a) $\hat{\rho}_{H1}$, (b) $\hat{v}_{2H1}$, (c) $\hat{T}_{H1}$.

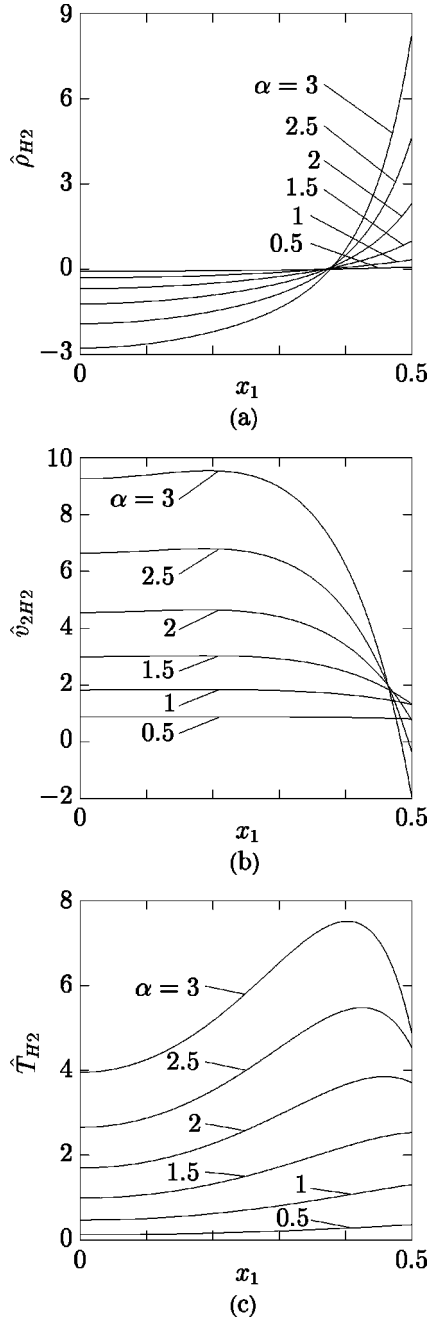

FIG. 3. The solution $\hat{\rho}_{H2}$, $\hat{v}_{2H2}$, and $\hat{T}_{H2}$ for various α. (a) $\hat{\rho}_{H2}$, (b) $\hat{v}_{2H2}$, (c) $\hat{T}_{H2}$.

Figures 4–6 show the profiles of the density ρ, flow velocity v_2, and temperature T for $\alpha=1$, 2, and 3 (i.e., $\hat{F}=$Kn, 2Kn, and 3Kn) in the right half ($0 \leqslant X_1/L \leqslant 0.5$) of the gap. Here, the solid line indicates the asymptotic solution up to the order of ϵ^2 (or Kn^2), i.e., $h=h_{H0}+(h_{H1}+h_{K1})\epsilon+(h_{H2}+h_{K2})\epsilon^2$ with $h=\hat{\rho}$, $\hat{v}_2$, or $\hat{T}$, whereas the dashed line the corresponding numerical solution of the original BGK model obtained by means of a finite-difference method, on which we will comment in the next section. The dimensional variables rather than the dimensionless counterparts are used in Figs. 4–6 [cf. Eq. (8)]. For $\alpha=2$ and 3, the discrepancy between the asymptotic and numerical solutions is appreciable in the figures at Kn$=0.1$, though their relative difference is still small (less than one percent). There are two reasons for this discrepancy. First, for $\alpha \geqslant 2$, the second-order Hilbert solution shown in Fig. 3 becomes large in magnitude compared with the leading and first-order solutions shown in Figs. 1 and 2. Second, the decay of the second-order Knudsen-layer functions is rather slow (see Table I), and further the magnitude of the second-order Knudsen-layer corrections in Eqs. (57a) and (57b) becomes large because they contain the square terms of $(d\hat{v}_{2H0}/dy)_B$ and $(d\hat{T}_{H0}/dy)_B$, which are large for larger α. Therefore, the Knudsen layer, which should be confined near the wall theo-

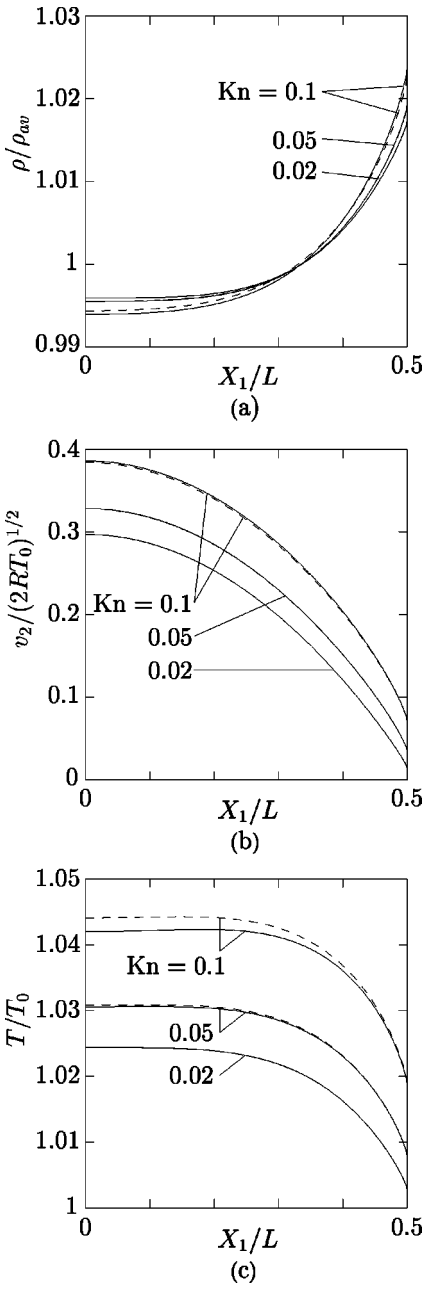

FIG. 4. The profiles of the density ρ, flow velocity v_2, and temperature T for Kn=0.02, 0.05, and 0.1 in the case of $\alpha=1$ [cf. Eq. (18)]. (a) ρ, (b) v_2, (c) T. The solid line indicates the asymptotic solution up to the order of Kn^2, and the dashed line the numerical solution of the original BGK system. These two lines are indistinguishable for Kn=0.02.

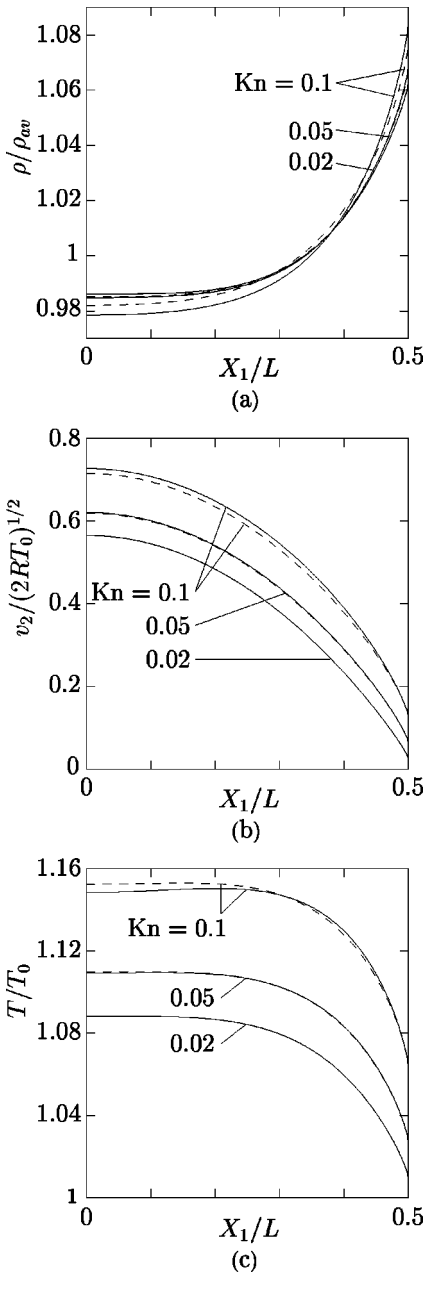

FIG. 5. The profiles of the density ρ, flow velocity v_2, and temperature T for Kn=0.02, 0.05, and 0.1 in the case of $\alpha=2$ [cf. Eq. (18)]. (a) ρ, (b) v_2, (c) T. See the caption of Fig. 4.

retically, almost reaches the center of the gap at Kn=0.1. These two facts restrict the validity of the asymptotic expansion to rather small values of Kn.

The numerical data corresponding to the temperature profile in Figs. 4–6 show that it is of a bimodal shape with a very slight local minimum at the center of the gap ($X_1=0$). This fact has been discussed in earlier works [2–7] (see Sec. I). To see this more clearly, we show in Fig. 7 magnified figures of the temperature profile in the central part of the gap in the case of Fig. 6(c) (i.e., $\alpha=3$). Such a bimodal shape is not observed in the solution up to the first order, i.e., $\hat{T}=\hat{T}_{H0}+(\hat{T}_{H1}+\hat{T}_{K1})\epsilon$. Therefore, it is a second-order effect. The presence of the local minimum at $X_1=0$ can be shown analytically. Because of the symmetry of the flow field with respect to the x_2 axis [Eq. (17)], we have $d^{2k+1}\hat{v}_{2Hm}/dx_1^{2k+1}=d^{2k+1}\hat{T}_{Hm}/dx_1^{2k+1}=0$ at $x_1=0$ ($k=0,1,...$). Therefore, Eqs. (31b), (31c) and (32c) give, respectively, $(d^2\hat{v}_{2H0}/dx_1^2)_{x_1=0}=-(4/\sqrt{\pi})\alpha\hat{\rho}_{H0}(0)/\hat{T}_{H0}(0)$, $(d^2\hat{T}_{H0}/dx_1^2)_{x_1=0}=0$, and $(d^2\hat{T}_{H1}/dx_1^2)_{x_1=0}=0$. Then, it follows from Eq. (33c) that $(d^2\hat{T}_{H2}/dx_1^2)_{x_1=0}=608\alpha^2/25\pi\hat{T}_{H0}(0)$. In summary, we have

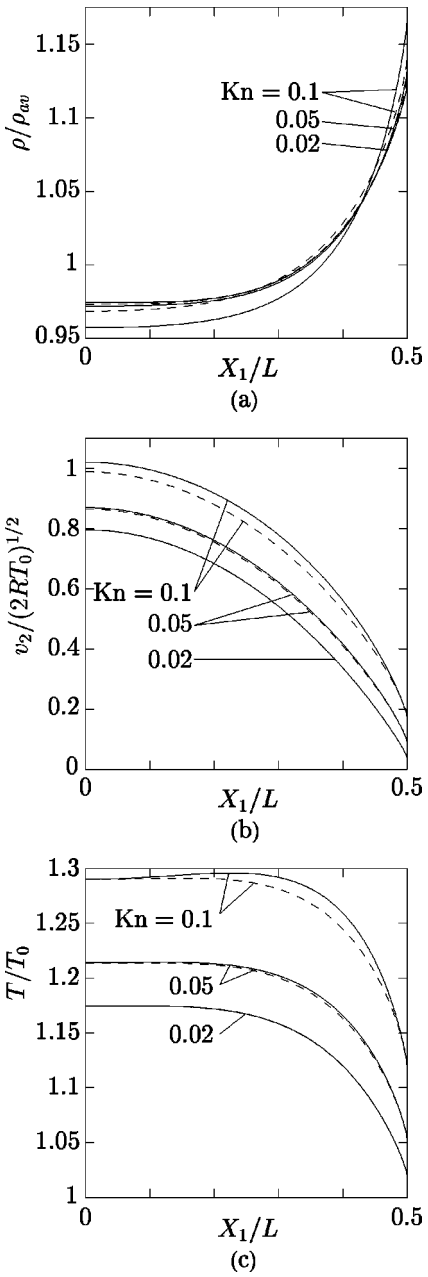

FIG. 6. The profiles of the density ρ, flow velocity v_2, and temperature T for Kn=0.02, 0.05, and 0.1 in the case of $\alpha=3$ [cf. Eq. (18)]. (a) ρ, (b) v_2, (c) T. See the caption of Fig. 4.

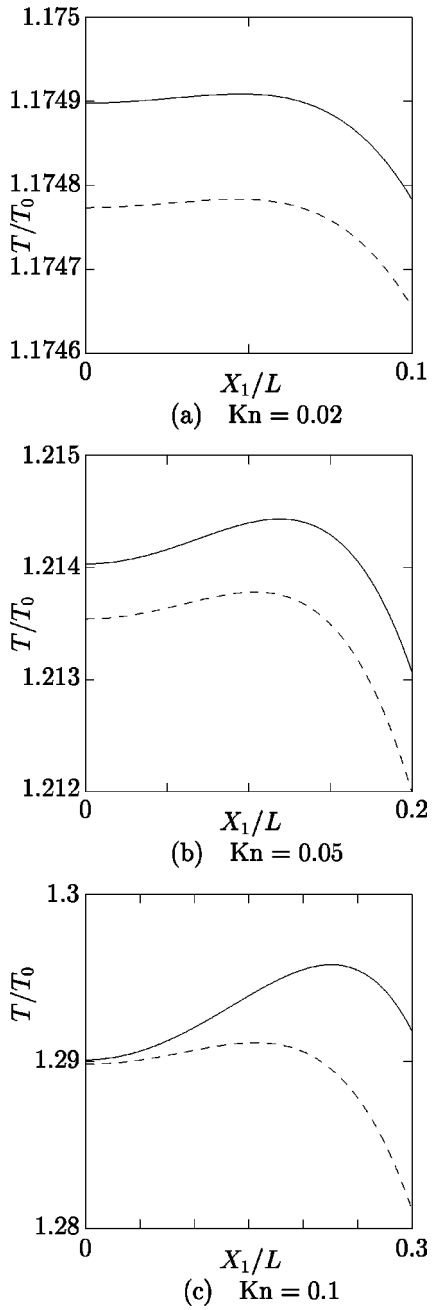

FIG. 7. The temperature profile in the central part of the gap for $\alpha=3$ [cf. Fig. 6(c)]. (a) Kn=0.02, (b) Kn=0.05, (c) Kn=0.1. The solid line indicates the asymptotic solution up to the order of Kn^2, and the dashed line the numerical solution of the original BGK system.

$$\left(\frac{d\hat{T}}{dx_1}\right)_{x_1=0}=0,$$

$$\left(\frac{d^2\hat{T}}{dx_1^2}\right)_{x_1=0}=\frac{608}{25\pi}\frac{1}{\hat{T}(0)}\alpha^2\epsilon^2+O(\epsilon^3)>0. \tag{61}$$

That is, the presence of the local minimum is attributed to the solution of the second-order fluid-dynamic-type equations (see Fig. 3). Equation (61) coincides with the result obtained by Tij and Santos [2] (see also Ref. [4]).

The nontrivial components p_{11}, p_{22}, p_{33}, and p_{12} of the stress tensor and those q_1 and q_2 of the heat-flow vector for $\alpha=1$, 2, and 3 in the right half of the gap are shown in Figs. 8–10. As in Figs. 4–7, the solid line indicates the asymptotic solution up to the order of ϵ^2 (or Kn^2), i.e., $h=h_{H0}+(h_{H1}+h_{K1})\epsilon+(h_{H2}+h_{K2})\epsilon^2$ with $h=\hat{p}_{ij}$ or $\hat{q}_i$, whereas the dashed line the corresponding numerical solution of the original BGK system. The dimensional variables are used also in Figs. 8–10 [cf. Eq. (8)]. The p_{11} is constant [Eq. (16a)], and its Knudsen-layer part vanishes identically (see

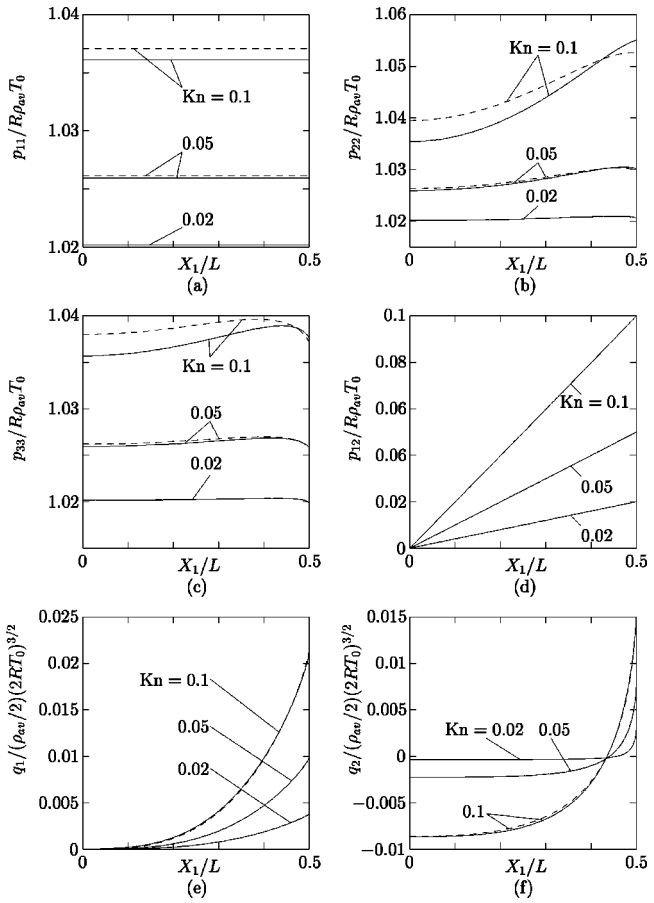

FIG. 8. The profiles of the nontrivial components of the stress tensor p_{ij} and the heat-flow vector q_i for Kn=0.02, 0.05, and 0.1 in the case of $\alpha=1$ [cf. Eq. (18)]. (a) p_{11}, (b) p_{22}, (c) p_{33}, (d) p_{12}, (e) q_1, (f) q_2. The solid line indicates the asymptotic solution up to the order of Kn^2, and the dashed line the numerical solution of the original BGK system. These two lines are indistinguishable for Kn=0.02.

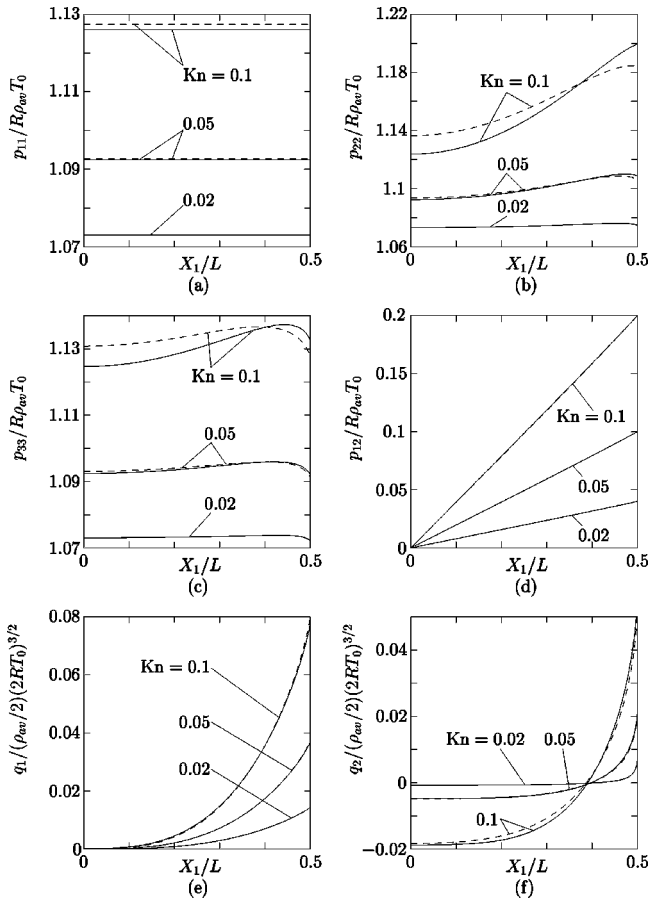

FIG. 9. The profiles of the nontrivial components of the stress tensor p_{ij} and the heat-flow vector q_i for Kn=0.02, 0.05, and 0.1 in the case of $\alpha=2$ [cf. Eq. (18)]. (a) p_{11}, (b) p_{22}, (c) p_{33}, (d) p_{12}, (e) q_1, (f) q_2. See the caption of Fig. 8.

Appendix D). As is seen from Eq. (16b), $p_{12}/R\rho_{\mathrm{av}}T_0=\pm\hat{F}=\pm\alpha\mathrm{Kn}$ at $X_1/L=\pm 1/2$. For the Navier-Stokes equation, the normal stresses $\hat{p}_{11}$, $\hat{p}_{22}$, and $\hat{p}_{33}$ are equal to the pressure $\hat{p}$, which is uniform, and there is no heat flow in the direction parallel to the walls ($\hat{q}_2=0$). In contrast, in the order of Kn^2, the pressure is not uniform [see Eq. (32a)], the normal stresses, which contain non-Navier-Stokes terms [the terms containing $\hat{T}_{H0}$ and $\hat{v}_{2H0}$ in Eqs. (C3a)–(C3c)], are not isotropic, and the heat flow parallel to the walls appear [see Eq. (C6b)]. These non-Navier-Stokes terms are of the form contained in the Burnett approximation [32] of the stress and heat flow. For the shear stress $\hat{p}_{12}$ and the heat flow $\hat{q}_1$ perpendicular to the walls, the non-Navier-Stokes terms appear in the order of Kn^3 (as mentioned in the end of Sec. III A, the explicit expressions of $\hat{p}_{ijH3}$ and $\hat{q}_{iH3}$ are omitted in this paper). These non-Navier-Stokes terms are not contained in the Burnett approximation. Therefore, it turns out that Eqs. (33b) and (33c), which include the contribution of $\hat{p}_{12H3}$ and $\hat{q}_{1H3}$, are affected by the terms beyond the Burnett approximation. As is seen from Figs. 8(f), 9(f), and 10(f), the heat flow $\hat{q}_2$ parallel to the walls changes its sign depending on the position in the gas. More specifically, it is in the direction of the gas flow near the walls but in the opposite direction in the middle. Similar change of the direction of the heat flow was noted in the ordinary Poiseuille flow driven by the pressure gradient [33].

We now give a short comment on the perturbation solution by Tij and Santos [2]. We have given some of the derivatives of $\hat{v}_{2Hm}$ and $\hat{T}_{Hm}$ at $x_1=0$ before Eq. (61). In addition, $d^{2k+1}\hat{p}_{Hm}/dx_1^{2k+1}=0$ holds at $x_1=0$ ($k=0,1,...$), and we obtain $(d^2\hat{p}_{H2}/dx_1^2)_{x_1=0}=192\alpha^2\hat{\rho}_{H0}(0)/5\pi\hat{T}_{H0}(0)$ from Eq. (32a). These results lead to the following Taylor series expansions of $\hat{v}_2$, $\hat{T}$, and $\hat{p}$ around $x_1=0$ when $|x_1|\lesssim\epsilon$.

$$\hat{v}_2=\hat{v}_2(0)-\frac{2}{\sqrt{\pi}}\frac{\hat{\rho}(0)}{\hat{T}(0)}\alpha x_1^2+O(\epsilon^3), \tag{62a}$$

$$\hat{T}=\hat{T}(0)-\frac{16}{15\pi}\frac{1}{\hat{T}(0)}\left[\frac{\hat{\rho}(0)^2}{\hat{T}(0)}x_1^2-\frac{57}{5}\epsilon^2\right]\alpha^2x_1^2+O(\epsilon^5), \tag{62b}$$

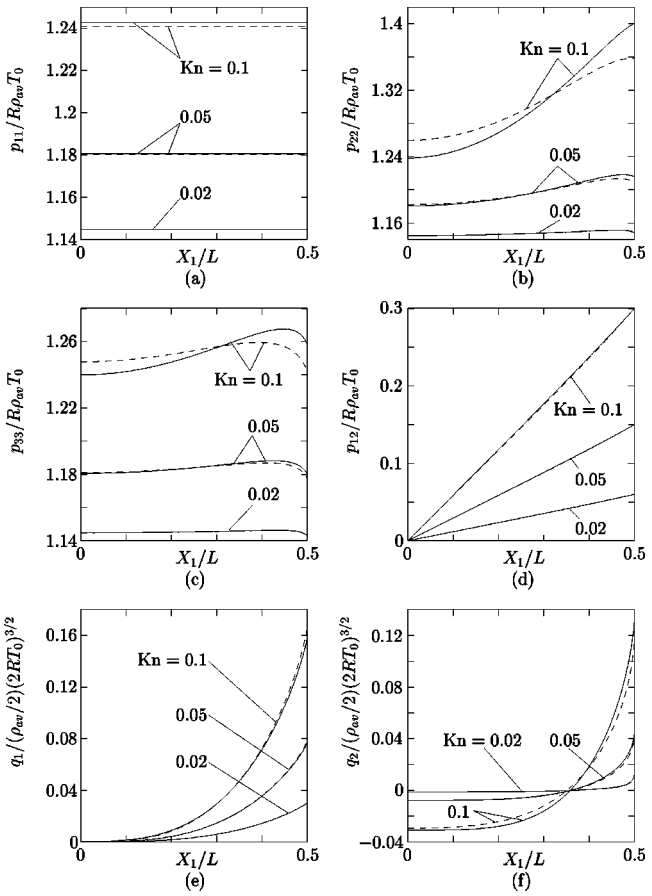

FIG. 10. The profiles of the nontrivial components of the stress tensor p_{ij} and the heat-flow vector q_i for Kn=0.02, 0.05, and 0.1 in the case of $\alpha=3$ [cf. Eq. (18)]. (a) p_{11}, (b) p_{22}, (c) p_{33}, (d) p_{12}, (e) q_1, (f) q_2. See the caption of Fig. 8.

$$\hat{p}=\hat{p}(0)+\frac{96}{5\pi}\frac{\hat{\rho}(0)}{\hat{T}(0)}\alpha^2\epsilon^2x_1^2+O(\epsilon^5). \tag{62c}$$

By a careful comparison, one can show that these results coincide with $u^{(1)}(s)F$, $1+T^{(2)}(s)F^2$, and $1+p^{(2)}(s)F^2$ in Ref. [2], respectively [cf. Eqs. (29)–(31), (33), (36), and (37) in Ref. [2]], if the higher-order terms are neglected. Therefore, it is most probable that the perturbation solution by Tij and Santos corresponds to the Taylor series expansion of the Hilbert (or normal) solution around the center of the gap, which is valid only in the vicinity of the center. Essentially the same agreement is observed for the stress tensor as well as the heat-flow vector. They were able to obtain higher-order terms, but their analysis cannot give any information about the values $\hat{v}_2(0)$, $\hat{T}(0)$, and $\hat{p}(0)$ at the center. Furthermore, it should be emphasized that the Hilbert solution can be regarded as a part of the solution of the boundary-value problem under consideration only when it can be consistently matched with the boundary condition through the Knudsen layer. In this sense, the present analysis would justify Tij and Santos' solution as a correct local solution near the center of the gap. They extended their analysis to the case of a circular pipe recently in Ref. [34], where the result for the flow between two plates is also summarized in a more tractable form than in Ref. [2].

As mentioned earlier, the present analysis completely follows the procedure of the asymptotic theory by Sone and co-workers [11–19]. Esposito, Lebowitz, and Marra [1] used a similar procedure to investigate the present problem for small ϵ in the case of the Boltzmann equation for hard-sphere molecules. Their aim is to clarify the mathematical structure of the solution rather than to obtain the flow field explicitly. They were able to obtain the estimates of the expanded terms and the remainder of the velocity distribution function and to show the convergence of the solution of the Boltzmann equation to that of the Navier-Stokes equation in the continuum limit $\epsilon\to 0$.

IV. NUMERICAL ANALYSIS FOR INTERMEDIATE KNUDSEN NUMBERS

In Sec. III B, we have already analyzed the Knudsen-layer problem (47a)–(47c) numerically by a finite-difference method. In addition, in Figs. 4–10, we have presented some numerical solutions of the original system, Eqs. (9)–(11c), (13), and (14), for small Knudsen numbers when the force parameter $\hat{F}$ is scaled as Eq. (18). In this section, we give some numerical results (numerical solutions of the original system) for intermediate values of the Knudsen number in the case where $\hat{F}$ is fixed. We first give a brief comment on the numerical solution method and then give results of analysis.

A. Some comments on the numerical method

In the numerical analysis, we can take advantage of the nice property of the BGK model that the ζ_2 and ζ_3 variables can be eliminated in spatially one-dimensional problems [35]. Let us introduce the following (dimensionless) marginal velocity distribution functions, which are the functions of x_1 and ζ_1:

$$\begin{bmatrix}\mathcal{G}_a\\ \mathcal{G}_b\\ \mathcal{G}_c\end{bmatrix}=\int_{-\infty}^{\infty}\int_{-\infty}^{\infty}\begin{bmatrix}1\\ \zeta_2\\ \zeta_2^2+\zeta_3^2\end{bmatrix}\hat{f}\,d\zeta_2 d\zeta_3. \tag{63}$$

By multiplying Eq. (9) by 1, ζ_2, and $\zeta_2^2+\zeta_3^2$ and integrating the respective equations over the whole range of ζ_2 and ζ_3, we obtain the simultaneous equations for $\mathcal{G}_a$, $\mathcal{G}_b$, and $\mathcal{G}_c$. The corresponding boundary conditions are derived by the same way from Eqs. (13) and (14). In summary, the resulting equations are given by

$$\zeta_1\frac{\partial}{\partial x_1}\begin{bmatrix}\mathcal{G}_a\\ \mathcal{G}_b\\ \mathcal{G}_c\end{bmatrix}-\hat{F}\begin{bmatrix}0\\ \mathcal{G}_a\\ 2\mathcal{G}_b\end{bmatrix}=\frac{2}{\sqrt{\pi}\mathrm{Kn}}\hat{\rho}\begin{bmatrix}\mathcal{G}_{ae}-\mathcal{G}_a\\ \mathcal{G}_{be}-\mathcal{G}_b\\ \mathcal{G}_{ce}-\mathcal{G}_c\end{bmatrix}, \tag{64}$$

where

$$\begin{bmatrix} \mathcal{G}_{ae} \\ \mathcal{G}_{be} \\ \mathcal{G}_{ce} \end{bmatrix} = \frac{\hat{\rho}}{(\pi\hat{T})^{1/2}} \exp\left(\frac{-\zeta_1^2}{\hat{T}}\right) \begin{bmatrix} 1 \\ \hat{v}_2 \\ \hat{v}_2^2+\hat{T} \end{bmatrix}, \tag{65}$$

$$\hat{\rho} = \int_{-\infty}^{\infty} \mathcal{G}_a d\zeta_1, \tag{66a}$$

$$\hat{v}_2 = (1/\hat{\rho}) \int_{-\infty}^{\infty} \mathcal{G}_b d\zeta_1, \tag{66b}$$

$$\hat{T} = (2/3\hat{\rho}) \int_{-\infty}^{\infty} [(\zeta_1^2+\hat{v}_2^2)\mathcal{G}_a - 2\hat{v}_2\mathcal{G}_b + \mathcal{G}_c] d\zeta_1, \tag{66c}$$

and the boundary conditions are given by

$$\begin{bmatrix} \mathcal{G}_a \\ \mathcal{G}_b \\ \mathcal{G}_c \end{bmatrix} = \frac{1}{\sqrt{\pi}} \hat{\rho}_w \exp(-\zeta_1^2) \begin{bmatrix} 1 \\ 0 \\ 1 \end{bmatrix}$$

$$\text{for} \quad \pm\zeta_1 > 0 \quad \text{at} \quad x_1 = \mp 1/2, \tag{67}$$

$$\hat{\rho}_w = \mp 2\sqrt{\pi} \int_{\pm\zeta_1<0} \zeta_1 \mathcal{G}_a(\mp 1/2, \zeta_1) d\zeta_1. \tag{68}$$

This system, in which the derivative term with respect to ζ_2 [cf. Eq. (9)] has disappeared, can be solved numerically by a finite-difference method in the same way as in Ref. [36], where half-space problems of strong condensation and evaporation are analyzed. Since the detailed description of the numerical method is found there, we omit it in the present paper. Because of the symmetry of the system (64)–(68) with respect to the x_2 axis, we carry out the actual computation in the half range $0 \leqslant x_1 \leqslant 1/2$ imposing the specular reflection condition for $\mathcal{G}_a$, $\mathcal{G}_b$, and $\mathcal{G}_c$ at $x_1 = 0$. It should be noted here that $\hat{p}_{22}$, $\hat{p}_{33}$, and $\hat{q}_2$ cannot be expressed in terms of the marginal velocity distribution functions $\mathcal{G}_a$, $\mathcal{G}_b$, and $\mathcal{G}_c$. However, once these are obtained, the $\hat{\rho}$, $\hat{v}_2$, and $\hat{T}$ and thus $\hat{f}_e$ in the original equation (9) are determined. Then, we can easily integrate Eq. (9) numerically with respect to x_1 under the boundary condition (13) to generate $\hat{f}$. In this way, we can compute $\hat{p}_{22}$, $\hat{p}_{33}$, and $\hat{q}_2$ easily. [In this process, one can also get rid of ζ_3 by introducing the marginal velocity distribution functions $\mathcal{F}_a = \int f d\zeta_3$ and $\mathcal{F}_b = \int \zeta_3^2 f d\zeta_3$ and using the equations and boundary conditions for them derived by the corresponding integrations of Eqs. (9) and (13).]

In Sec. III B, we carried out a numerical analysis of the Knudsen-layer problem (47a)–(47c) to determine the slip coefficients as well as the Knudsen-layer corrections. In this analysis, the elimination of ζ_2 and ζ_3 mentioned above has also been made. That is, we introduce three marginal velocity distribution functions $\mathcal{H}_{am}$, $\mathcal{H}_{bm}$, and $\mathcal{H}_{cm}$ of Φ_m defined respectively by $\mathcal{G}_a$, $\mathcal{G}_b$, and $\mathcal{G}_c$ with $\hat{f}$ replaced by $\Phi_m E$ in Eq. (63). Then the decomposition (51) is automatically made, i.e., $\mathcal{H}_b$, which contains only Φ_m^o, is decoupled from $\mathcal{H}_a$ and $\mathcal{H}_c$ containing only Φ_m^e. Then the resulting boundary-value problems for $\mathcal{H}_b$ and those for $(\mathcal{H}_a, \mathcal{H}_c)$ were solved numerically by a finite-difference method similar to that used for solving Eqs. (64)–(68). The slip coefficients associated with $\mathcal{H}_b$ (i.e., β_{1a}, β_{2b}, β_{2c}, and β_{2d}) were determined in the same way as in Ref. [30], while those associated with $(\mathcal{H}_a, \mathcal{H}_c)$ (i.e., $\tilde{\beta}_{1a}$, $\tilde{\beta}_{2b}$, $\tilde{\beta}_{2c}$, and $\tilde{\beta}_{2d}$) were determined in the same way as in Ref. [37].

B. Results of numerical analysis

Before presenting the results of numerical analysis, we give the solution for the free-molecular flow (Kn$=\infty$), that is,

$$\hat{f} = \frac{1}{\pi^{3/2}} \exp\left(-\zeta_1^2 - \left[\zeta_2 - \left(x_1 \pm \frac{1}{2}\right)\frac{\hat{F}}{\zeta_1}\right]^2 - \zeta_3^2\right) \quad (\pm\zeta_1 > 0), \tag{69a}$$

$$\hat{\rho} = 1, \quad \hat{v}_2 \to \infty, \quad \hat{T} \to \infty,$$

$$\hat{p}_{11} = \hat{p}_{33} = 1, \quad \hat{p}_{22} \to \infty, \quad \hat{p}_{12} = 2x_1\hat{F}, \tag{69b}$$

$$\hat{q}_1 = 0, \quad \hat{q}_2 \to \infty.$$

Here, we compute the macroscopic variables by integrating over a truncated ζ_i space with $-\infty < \zeta_1 < -\delta$ and $\delta < \zeta_1 < \infty$ ($\delta > 0$) and then taking the limit as $\delta \to 0$. In this limit, $\hat{v}_2$, $\hat{T}$, $\hat{p}_{22}$, and $\hat{q}_2$ diverge to (plus) infinity.

In Figs. 11 and 12, we show the profiles of the density, flow velocity, and temperature for various Knudsen numbers for two fixed values of the force parameter $\hat{F}$ [Eq. (12a)], i.e., $\hat{F} = 0.05$ (Fig. 11) and $\hat{F} = 0.5$ (Fig. 12). In the former case where $\hat{F}$ is small, the flow speed is naturally lower, and thus the nonuniformity in the density and temperature is smaller compared with the latter case. For $\hat{F} = 0.5$ (Fig. 12), a high-speed flow is caused for small Kn [note that $v_2/(2RT_0)^{1/2} = \sqrt{5/6}$ corresponds to the sonic speed], and correspondingly the variation in the density and temperature becomes large. For large Kn, the profiles tend to become uniform. As Kn increases from small values, the flow speed in the bulk of the gas decreases, becomes lowest at intermediate values of Kn [Kn$\simeq 1$ in Figs. 11(b) and 12(b)], and then increases. As shown in Eq. (69b), the flow speed becomes infinity as Kn$\to\infty$. On the other hand, for any fixed value of $\hat{F}$, the flow speed increases indefinitely as Kn approaches zero. In order for the flow speed to remain finite in the limit Kn$\to 0$ (continuum limit), the force parameter $\hat{F}$ should be of the order of Kn [cf. Eq. (18)], as we have seen in Sec. III. The temperature in Figs. 11(c) and 12(c) also becomes lowest at intermediate values of Kn, corresponding to the behavior of the flow speed.

Figures 13 and 14 show the profiles of the nontrivial components of the stress tensor and the heat-flow vector for various Knudsen numbers for $\hat{F} = 0.05$ (Fig. 13) and 0.5 (Fig. 14). The result for Kn$=10$, which ranges from 4.3631 to 4.7845, is omitted in Fig. 14(b); and the results for Kn$=5$ and 10, which range from 2.5637 to 3.1487 and from 10.762

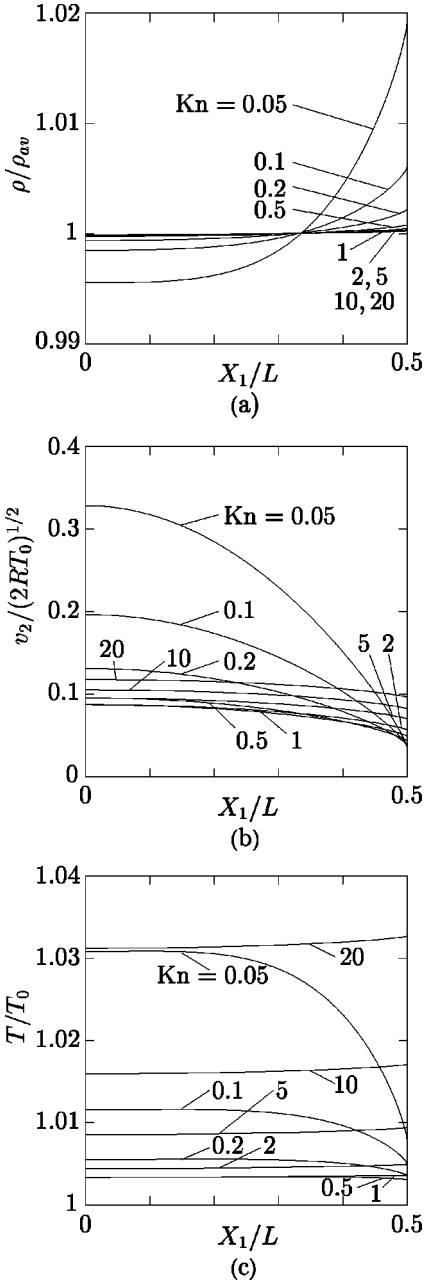

FIG. 11. The profiles of the density ρ, flow velocity v_2, and temperature T for various Kn in the case of $\hat{F}=0.05$. (a) ρ, (b) v_2, (c) T.

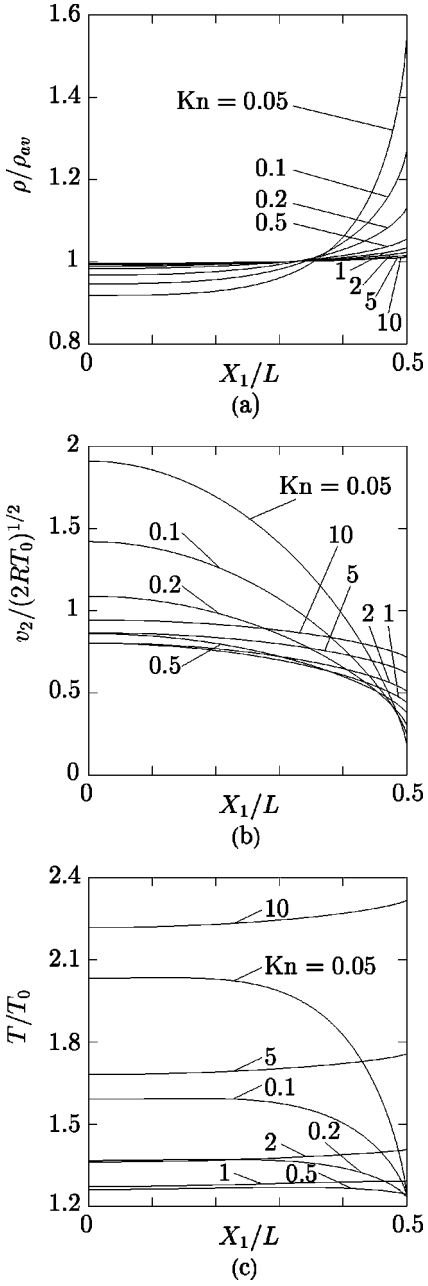

FIG. 12. The profiles of the density ρ, flow velocity v_2, and temperature T for various Kn in the case of $\hat{F}=0.5$. (a) ρ, (b) v_2, (c) T.

to 11.732, respectively, are omitted in Fig. 14(f). The p_{11} is independent of X_1 [Eq. (16a)], and $p_{12}/R\rho_{\rm av}T_0$ is almost independent of Kn [Figs. 13(d) and 14(d)]. Figures 13(f) and 14(f) show the change of the sign of q_2 (the component of the heat-flow vector parallel to the wall) depending on the position in the gas for small Kn, as in the case of Figs. 8(f), 9(f), and 10(f). As Kn increases from small values, q_2 decreases, becomes smallest at intermediate values of Kn [Kn $=5$ in Fig. 13(f) and Kn$=0.5$ in Fig. 14(f)], and then increases. For $\hat{F}=0.05$, q_2 is negative in the whole gap for a wide range of Kn (at least for $0.5\leqslant$Kn$\leqslant 10$). The approach of the physical quantities to the free-molecular flow values (69b) is rather slow.

Figure 15 and Table II show the mass flow $\mathcal{M}$ and the heat flow $\mathcal{Q}$ in the X_2 direction per unit width in X_3 and per unit time, i.e.,

$$\mathcal{M}=\int_{-L/2}^{L/2}\rho v_2 dX_1=2\rho_{\rm av}(2RT_0)^{1/2}L\int_0^{1/2}\hat{\rho}\hat{v}_2 dx_1, \tag{70a}$$

$$\mathcal{Q}=\int_{-L/2}^{L/2}q_2 dX_1=\rho_{\rm av}(2RT_0)^{3/2}L\int_0^{1/2}\hat{q}_2 dx_1, \tag{70b}$$

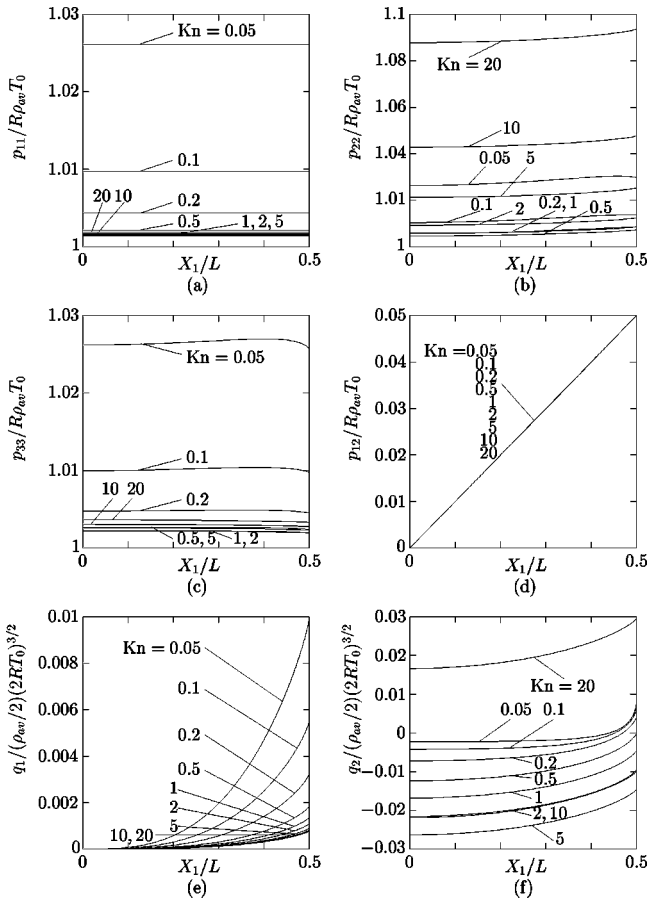

FIG. 13. The profiles of the nontrivial components of the stress tensor p_{ij} and the heat-flow vector q_i for various Kn in the case of $\hat{F}=0.05$. (a) p_{11}, (b) p_{22}, (c) p_{33}, (d) p_{12}, (e) q_1, (f) q_2.

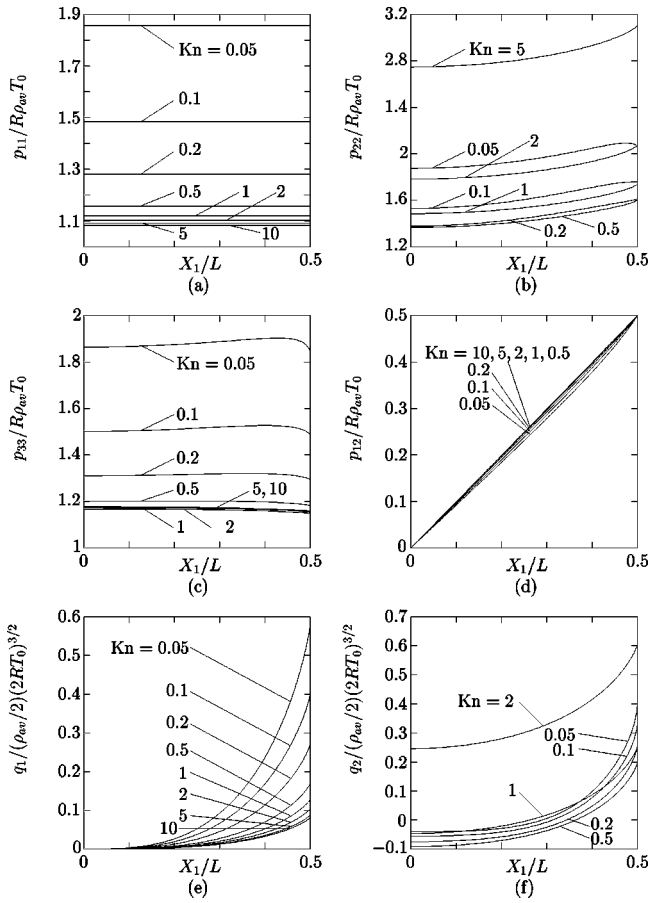

FIG. 14. The profiles of the nontrivial components of the stress tensor p_{ij} and the heat-flow vector q_i for various Kn in the case of $\hat{F}=0.5$. (a) p_{11}, (b) p_{22}, (c) p_{33}, (d) p_{12}, (e) q_1, (f) q_2.

versus the Knudsen number for $\hat{F}=0.05$ [Fig. 15(a)] and 0.5 [Fig. 15(b)]. The corresponding results obtained from the asymptotic analysis for small Kn in Sec. III are also shown in Fig. 15(a) as well as in Table II. The dimensionless mass-flow rate $\mathcal{M}/2\rho_{\rm av}(2RT_0)^{1/2}L$ takes the minimum at an intermediate Knudsen number, which is similar to the Knudsen minimum [38] in the case of the Poiseuille flow caused by the pressure gradient [33]. It increases indefinitely in the limit $\mathrm{Kn}\to\infty$ as well as in the other limit $\mathrm{Kn}\to 0$, but the increase in the former is slow. The global heat flow changes its direction depending on the Knudsen number, that is, it is in the direction opposite to the flow in the range approximately $\mathrm{Kn}<15$ for $\hat{F}=0.05$ and in the range approximately $0.15<\mathrm{Kn}<0.8$ for $\hat{F}=0.5$, but in the direction of the flow in the other range. The increase of the dimensionless heat-flow rate $\mathcal{Q}/\rho_{\rm av}(2RT_0)^{3/2}L$ with Kn after it takes the (negative) minimum value is steep. It becomes infinitely large in the free-molecular flow limit.

V. DISCUSSIONS

In the present paper, we have investigated a Poiseuille-type flow of a rarefied gas between two parallel plates driven by an external force in the direction parallel to the wall. The basic system used here is the BGK model of the Boltzmann equation and the diffuse reflection boundary condition. First, the case of small Knudsen numbers was investigated by means of a systematic asymptotic analysis of the basic system for weak external force [Eq. (18)] (Sec. III). As a result, the fluid-dynamic type equations and their boundary conditions of slip type were obtained up to the second order in the Knudsen number, together with the Knudsen-layer corrections near the walls. Then, the original BGK system was analyzed numerically by an accurate finite-difference method

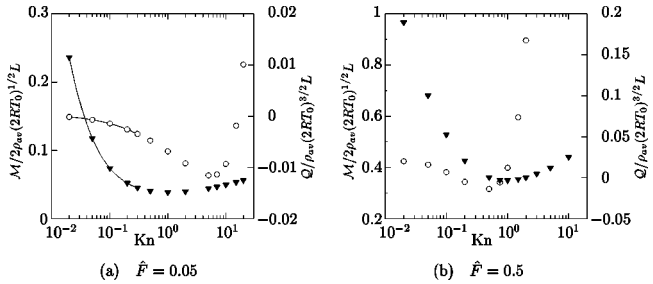

FIG. 15. The mass-flow rate $\mathcal{M}$ and the heat-flow rate $\mathcal{Q}$ vs Kn. (a) $\hat{F}=0.05$, (b) $\hat{F}=0.5$. Here, ▼ indicates the mass-flow rate, ○ the heat-flow rate, and the solid line the corresponding results based on the asymptotic analysis in Sec. III.

TABLE II. Mass and heat-flow rates. The values in the parentheses indicate the results based on the asymptotic analysis in Sec. III.

	$\mathcal{M}/2\rho_{\rm av}(2RT_0)^{1/2}L$		$\mathcal{Q}/\rho_{\rm av}(2RT_0)^{3/2}L$	
Kn	$\hat{F}=0.05$	$\hat{F}=0.5$	$\hat{F}=0.05$	$\hat{F}=0.5$
0.02	2.361×10^{-1}	9.659×10^{-1}	-1.360×10^{-4}	2.010×10^{-2}
	(2.362×10^{-1})		(-1.248×10^{-4})	
0.05	1.176×10^{-1}	6.806×10^{-1}	-7.089×10^{-4}	1.583×10^{-2}
	(1.178×10^{-1})		(-7.081×10^{-4})	
0.1	7.374×10^{-2}	5.280×10^{-1}	-1.445×10^{-3}	6.680×10^{-3}
	(7.385×10^{-2})		(-1.452×10^{-3})	
0.2	5.198×10^{-2}	4.262×10^{-1}	-2.584×10^{-3}	-5.201×10^{-3}
	(5.197×10^{-2})		(-2.600×10^{-3})	
0.3	4.520×10^{-2}		-3.461×10^{-3}	
	(4.490×10^{-2})		(-3.478×10^{-3})	
0.5	4.047×10^{-2}	3.603×10^{-1}	-4.775×10^{-3}	-1.385×10^{-2}
0.75		3.506×10^{-1}		-5.791×10^{-3}
1	3.841×10^{-2}	3.492×10^{-1}	-6.875×10^{-3}	1.206×10^{-2}
1.5		3.535×10^{-1}		7.371×10^{-2}
2	3.955×10^{-2}	3.603×10^{-1}	-9.195×10^{-3}	1.676×10^{-1}
3		3.743×10^{-1}		4.477×10^{-1}
5	4.428×10^{-2}	3.982×10^{-1}	-1.158×10^{-2}	1.358×10^{0}
7	4.671×10^{-2}		-1.138×10^{-2}	
10	4.961×10^{-2}	4.400×10^{-1}	-9.317×10^{-3}	5.509×10^{0}
15	5.327×10^{-2}		-1.877×10^{-3}	
20	5.606×10^{-2}		1.010×10^{-2}	

for intermediate as well as small Knudsen numbers (Sec. IV). The numerical results for small Knudsen numbers were compared with the results obtained by the fluid-dynamic-type systems (Sec. III).

The analysis of Sec. III shows that the non-Navier-Stokes effects (other than the slip boundary conditions) manifest themselves in the second order in the Knudsen number. For example, the anisotropy of the normal stress p_{11}, p_{22}, and p_{33} and the heat flow q_2 in the direction of the flow appear in this order. The bimodal shape with a very slight local minimum at the center of the gap in the temperature profile is also attributed to the effect of the second-order temperature field.

Finally, let us consider the continuum limit, where the Knudsen number vanishes, on the basis of the result obtained in Sec. III. In this limit, the parameter $\hat{F}$, which is a measure of the external force, vanishes because of the setting of Eq. (18). Therefore, one may think that the present problem reduces to the case of a gas between two plates at rest (with a common temperature) in the absence of an external force and in consequence the gas is at rest. But it is not true. In this limit, the flow field in the present problem approaches the leading-order terms of the Hilbert expansion [Eqs. (19) and (20)], i.e., $\hat{\rho}\to\hat{\rho}_{H0}$, $\hat{T}\to\hat{T}_{H0}$, $\hat{v}_2\to\hat{v}_{2H0}$, etc. That is, the flow does not vanish in this limit, and the flow field depends on the coefficient α in Eq. (18). In other words, a vanishingly weak external force can cause a gas flow with a rather high speed in the continuum limit. For instance, $|v_2|_{\max}/(2RT_0)^{1/2}\simeq0.28$ for $\alpha=1$ and $|v_2|_{\max}/(2RT_0)^{1/2}\simeq0.75$ for $\alpha=3$ [see Fig. 1(b); note that $(2RT_0)^{1/2}$ is nearly the sound speed]. The cause of this seemingly paradoxical result can be explained on the basis of the Navier-Stokes equation. In the present unidirectional flow, the flow field is essentially determined by the balance of two terms: the viscosity term $(1/\rho)d(\mu dv_2/dX_1)/dX_1$ and the external-force term F_2. The former is of the order of $(2RT_0/L)[U/(2RT_0)^{1/2}]$Kn, where U is the reference flow speed, because $\mu/\rho\sim(2RT_0)^{1/2}l_0$. Therefore, if F_2 is of the order of $(2RT_0/L)$Kn or $\hat{F}\sim$Kn [Eq. (18)], then the external-force term is balanced by the viscosity term with a finite U or $U\sim(2RT_0)^{1/2}$, i.e., with a flow of a finite Mach number. The situation remains unchanged in the limit Kn $\to0$ because Kn cancels out from both terms. In this way, a vanishingly weak external force can cause a flow of a finite Mach number.

Here we recall that the present problem is originally characterized by the two independent dimensionless parameters $\hat{F}$ and Kn [Eq. (12)] and that the continuum limit discussed above is based on the setting $\hat{F}\sim$Kn [Eq. (18)] between $\hat{F}$ and Kn. What happens in the continuum limit when one imposes the condition $\hat{F}\sim1$ (that is, $\hat{F}$ is independent of Kn) or $\hat{F}=o$(Kn) is now obvious. When $\hat{F}\sim1$ (i.e., $F_2\sim2RT_0/L$), the flow speed should be $U/(2RT_0)^{1/2}\sim1/$Kn, so that it increases indefinitely as Kn$\to0$. When $\hat{F}=o$(Kn), the flow speed should be $U/(2RT_0)^{1/2}=o(1)$ and thus vanishes in the limit Kn$\to0$. In this case, the solution

approaches that in the case without an external force.

The balance between the terms that are of the order of Kn (in an appropriate scaling) and thus vanish in the continuum limit [such as the viscosity term with $U\sim(2RT_0)^{1/2}$ and the external-force term discussed above] results in the fact that the behavior in the continuum limit can be affected by vanishingly small quantities in this limit. Such an effect is called the *ghost* effect. In the present problem, this effect could be explained in the framework of the classical Navier-Stokes equations (see the preceding paragraphs). But, in general, it cannot be described by the Navier-Stokes system (more specifically, the conservation equations of mass, momentum, and energy with Newton's law of stress and Fourier's law of heat flow and the nonslip boundary condition for the velocity and temperature) because, except for the viscosity and heat-conduction terms, the effects of the order of Kn (such as the thermal creep flow [30,39–41] and the nonlinear thermal stress flow [15,42,43]) are not contained in the system. As an example, let us consider a gas in a closed container at rest with an arbitrarily assigned surface temperature varying along the surface in the absence of external forces. If we investigate the steady behavior of the gas using the Navier-Stokes system, we are led to the conclusion that the gas is at rest and the temperature distribution in the gas is described by the steady heat-conduction equation with the nonjump condition. However, the second part of the conclusion is not true except for some special cases. In reality, the thermal creep and nonlinear thermal stress flows, which vanish in the continuum limit, give a significant effect on the temperature field in this limit. Therefore, the Navier-Stokes system has a serious defect in describing the behavior of the gas even in the continuum limit, in spite of the fact that it is generally accepted as the correct system for this limit. This fact was pointed out in Ref. [15]. The reader is referred to Refs. [19], [44–47] in addition to Ref. [15] for the details and further discussions.

It should be noted that we do not need to follow the aforementioned limiting process to the continuum limit by experiments. If the parameters of the experiment being performed are close to the limit, then we can predict the result of the experiment from that of the limit. For instance, suppose that a two-dimensional vertical channel with width 5 cm and length, say 10 m, connects two large reservoirs separated vertically and that the pressures of the gas in the two reservoirs are regulated in such a way that the pressure at the channel entrance in each reservoir is exactly the same. Then, the gas flows downward through the channel because of the gravity. Suppose that the gas is argon, the pressure is 1 atm, and the gravity is that on the earth. Then, the Knudsen number is $\mathrm{Kn}\simeq 1.8\times 10^{-6}$ and the force parameter is $\hat{F}\simeq 4\times 10^{-6}$. This is nearly the continuum limit and satisfies the condition (18) with $\alpha\simeq 2.2$. Therefore, one can predict that the Mach number of the gas flow reaches 0.6 at the center of the channel.

ACKNOWLEDGMENTS

This work was motivated by the discussions with Professor A. Santos while he was visiting Kyoto University as a visiting fellow (short term) of the Japan Society for the Promotion of Science. The authors wish to thank him for his valuable discussions and comments.

APPENDIX A: HILBERT EXPANSION OF THE MACROSCOPIC QUANTITIES

In this appendix, we summarize explicit expressions of the coefficients h_{Hm} in terms of $\hat{f}_{Hm}$ for $\hat{\rho}_H$, $\hat{v}_{2H}$, $\hat{T}_H$, $\hat{p}_H$, $\hat{p}_{ijH}$, and $\hat{q}_{iH}$ up to $m=2$.

$$\hat{\rho}_{H0}=\int \hat{f}_{H0}\,d\boldsymbol{\zeta}, \tag{A1a}$$

$$\hat{v}_{2H0}=(1/\hat{\rho}_{H0})\int \zeta_2\hat{f}_{H0}\,d\boldsymbol{\zeta}, \tag{A1b}$$

$$\hat{T}_{H0}=(2/3\hat{\rho}_{H0})\int [\zeta_1^2+(\zeta_2-\hat{v}_{2H0})^2+\zeta_3^2]\hat{f}_{H0}\,d\boldsymbol{\zeta}, \tag{A1c}$$

$$\hat{p}_{H0}=\hat{\rho}_{H0}\hat{T}_{H0}, \tag{A1d}$$

$$\hat{p}_{ijH0}=2\int (\zeta_i-\hat{v}_{2H0}\delta_{i2})(\zeta_j-\hat{v}_{2H0}\delta_{j2})\hat{f}_{H0}\,d\boldsymbol{\zeta}, \tag{A1e}$$

$$\hat{q}_{iH0}=\int (\zeta_i-\hat{v}_{2H0}\delta_{i2})[\zeta_1^2+(\zeta_2-\hat{v}_{2H0})^2+\zeta_3^2]\hat{f}_{H0}\,d\boldsymbol{\zeta}, \tag{A1f}$$

$$\hat{\rho}_{H1}=\int \hat{f}_{H1}\,d\boldsymbol{\zeta}, \tag{A2a}$$

$$\hat{v}_{2H1}=(1/\hat{\rho}_{H0})\int \zeta_2\hat{f}_{H1}\,d\boldsymbol{\zeta}-(\hat{\rho}_{H1}/\hat{\rho}_{H0})\hat{v}_{2H0}, \tag{A2b}$$

$$\hat{T}_{H1}=(2/3\hat{\rho}_{H0})\int [\zeta_1^2+(\zeta_2-\hat{v}_{2H0})^2+\zeta_3^2]\hat{f}_{H1}\,d\boldsymbol{\zeta} -(\hat{\rho}_{H1}/\hat{\rho}_{H0})\hat{T}_{H0}, \tag{A2c}$$

$$\hat{p}_{H1}=\hat{\rho}_{H0}\hat{T}_{H1}+\hat{\rho}_{H1}\hat{T}_{H0}, \tag{A2d}$$

$$\hat{p}_{ijH1}=2\int (\zeta_i-\hat{v}_{2H0}\delta_{i2})(\zeta_j-\hat{v}_{2H0}\delta_{j2})\hat{f}_{H1}\,d\boldsymbol{\zeta}, \tag{A2e}$$

$$\hat{q}_{iH1}=\int (\zeta_i-\hat{v}_{2H0}\delta_{i2})[\zeta_1^2+(\zeta_2-\hat{v}_{2H0})^2+\zeta_3^2]\hat{f}_{H1}\,d\boldsymbol{\zeta} -(\hat{p}_{i2H0}+\tfrac{3}{2}\hat{p}_{H0}\delta_{i2})\hat{v}_{2H1}, \tag{A2f}$$

$$\hat{\rho}_{H2}=\int \hat{f}_{H2}\,d\boldsymbol{\zeta}, \tag{A3a}$$

$$\hat{v}_{2H2}=(1/\hat{\rho}_{H0})\int \zeta_2\hat{f}_{H2}\,d\boldsymbol{\zeta}-(\hat{\rho}_{H1}/\hat{\rho}_{H0})\hat{v}_{2H1} -(\hat{\rho}_{H2}/\hat{\rho}_{H0})\hat{v}_{2H0}, \tag{A3b}$$

$$\hat{T}_{H2}=(2/3\hat{\rho}_{H0})\int[\zeta_1^2+(\zeta_2-\hat{v}_{2H0})^2+\zeta_3^2]\hat{f}_{H2}d\boldsymbol{\zeta}$$
$$-(\hat{\rho}_{H1}/\hat{\rho}_{H0})\hat{T}_{H1}-(\hat{\rho}_{H2}/\hat{\rho}_{H0})\hat{T}_{H0}-(2/3)\hat{v}_{2H1}^2, \tag{A3c}$$

$$\hat{p}_{H2}=\hat{\rho}_{H0}\hat{T}_{H2}+\hat{\rho}_{H1}\hat{T}_{H1}+\hat{\rho}_{H2}\hat{T}_{H0}, \tag{A3d}$$

$$\hat{p}_{ijH2}=2\int(\zeta_i-\hat{v}_{2H0}\delta_{i2})(\zeta_j-\hat{v}_{2H0}\delta_{j2})\hat{f}_{H2}d\boldsymbol{\zeta}$$
$$-2\hat{\rho}_{H0}\hat{v}_{2H1}^2\delta_{i2}\delta_{j2}, \tag{A3e}$$

$$\hat{q}_{iH2}=\int(\zeta_i-\hat{v}_{2H0}\delta_{i2})[\zeta_1^2+(\zeta_2-\hat{v}_{2H0})^2+\zeta_3^2]\hat{f}_{H2}d\boldsymbol{\zeta}$$
$$-(\hat{p}_{i2H0}+\tfrac{3}{2}\hat{p}_{H0}\delta_{i2})\hat{v}_{2H2}-(\hat{p}_{i2H1}+\tfrac{3}{2}\hat{p}_{H1}\delta_{i2})\hat{v}_{2H1}, \tag{A3f}$$

where δ_{ij} is the Kronecker delta. Note that $\hat{p}_{13Hm}=\hat{p}_{23Hm}=0$ and $\hat{q}_{3Hm}=0$.

APPENDIX B: HILBERT EXPANSION OF THE LOCAL MAXWELLIAN

The coefficients $\hat{f}_{eH0}$, $\hat{f}_{eH1}$, and $\hat{f}_{eH2}$ in Eq. (21) are summarized in the following:

$$\hat{f}_{eH0}=\frac{\hat{\rho}_{H0}}{(\pi\hat{T}_{H0})^{3/2}}\exp\left(-\frac{\zeta_1^2+(\zeta_2-\hat{v}_{2H0})^2+\zeta_3^2}{\hat{T}_{H0}}\right), \tag{B1a}$$

$$\hat{f}_{eH1}=\hat{f}_{eH0}\left[\frac{\hat{\rho}_{H1}}{\hat{\rho}_{H0}}+2\frac{(\zeta_2-\hat{v}_{2H0})\hat{v}_{2H1}}{\hat{T}_{H0}}\right.$$
$$\left.+\left(\frac{\zeta_1^2+(\zeta_2-\hat{v}_{2H0})^2+\zeta_3^2}{\hat{T}_{H0}}-\frac{3}{2}\right)\frac{\hat{T}_{H1}}{\hat{T}_{H0}}\right], \tag{B1b}$$

$$\hat{f}_{eH2}=\hat{f}_{eH0}\left\{\frac{\hat{\rho}_{H2}}{\hat{\rho}_{H0}}+2\frac{(\zeta_2-\hat{v}_{2H0})\hat{v}_{2H2}}{\hat{T}_{H0}}\right.$$
$$+\left(\frac{\zeta_1^2+(\zeta_2-\hat{v}_{2H0})^2+\zeta_3^2}{\hat{T}_{H0}}-\frac{3}{2}\right)\frac{\hat{T}_{H2}}{\hat{T}_{H0}}$$
$$+\frac{1}{2}\left[\frac{\hat{\rho}_{H1}}{\hat{\rho}_{H0}}+2\frac{(\zeta_2-\hat{v}_{2H0})\hat{v}_{2H1}}{\hat{T}_{H0}}\right.$$
$$\left.\left.+\left(\frac{\zeta_1^2+(\zeta_2-\hat{v}_{2H0})^2+\zeta_3^2}{\hat{T}_{H0}}-\frac{3}{2}\right)\frac{\hat{T}_{H1}}{\hat{T}_{H0}}\right]^2\right.$$
$$\left.-\frac{1}{2}\left(\frac{\hat{\rho}_{H1}}{\hat{\rho}_{H0}}\right)^2-2\frac{(\zeta_2-\hat{v}_{2H0})\hat{v}_{2H1}}{\hat{T}_{H0}^2}\hat{T}_{H1}\right.$$
$$\left.-\left(\frac{\zeta_1^2+(\zeta_2-\hat{v}_{2H0})^2+\zeta_3^2}{\hat{T}_{H0}}-\frac{3}{4}\right)\left(\frac{\hat{T}_{H1}}{\hat{T}_{H0}}\right)^2-\frac{\hat{v}_{2H1}^2}{\hat{T}_{H0}}\right\}. \tag{B1c}$$

APPENDIX C: STRESS TENSOR AND HEAT-FLOW VECTOR OF THE HILBERT SOLUTION

In this appendix, we summarize the expressions of the coefficients $\hat{p}_{ijHm}$ and $\hat{q}_{iHm}$ of the Hilbert expansion (20) of the stress tensor $\hat{p}_{ij}$ and that of the heat-flow vector $\hat{q}_i$ in terms of $\hat{p}_{Hn}$, $\hat{T}_{Hn}$, and $\hat{v}_{2Hn}(n\leqslant m)$ for $m=0$, 1, and 2; that is,

$$\hat{p}_{11H0}=\hat{p}_{22H0}=\hat{p}_{33H0}=\hat{p}_{H0},$$
$$\hat{p}_{12H0}=\hat{p}_{21H0}=0, \tag{C1}$$

$$\hat{p}_{11H1}=\hat{p}_{22H1}=\hat{p}_{33H1}=\hat{p}_{H1},$$
$$\hat{p}_{12H1}=\hat{p}_{21H1}=-\hat{T}_{H0}\frac{d\hat{v}_{2H0}}{dx_1}, \tag{C2}$$

$$\hat{p}_{11H2}=\hat{p}_{H2}+\frac{3}{2}\frac{1}{\hat{\rho}_{H0}}\frac{d}{dx_1}\left(\hat{T}_{H0}\frac{d\hat{T}_{H0}}{dx_1}\right), \tag{C3a}$$

$$\hat{p}_{22H2}=\hat{p}_{H2}+\frac{1}{2}\frac{1}{\hat{\rho}_{H0}}\frac{d}{dx_1}\left(\hat{T}_{H0}\frac{d\hat{T}_{H0}}{dx_1}\right)+2\frac{\hat{T}_{H0}}{\hat{\rho}_{H0}}\left(\frac{d\hat{v}_{2H0}}{dx_1}\right)^2, \tag{C3b}$$

$$\hat{p}_{33H2}=\hat{p}_{H2}+\frac{1}{2}\frac{1}{\hat{\rho}_{H0}}\frac{d}{dx_1}\left(\hat{T}_{H0}\frac{d\hat{T}_{H0}}{dx_1}\right), \tag{C3c}$$

$$\hat{p}_{12H2}=\hat{p}_{21H2}=-\hat{T}_{H1}\frac{d\hat{v}_{2H0}}{dx_1}-\hat{T}_{H0}\frac{d\hat{v}_{2H1}}{dx_1}, \tag{C3d}$$

$$\hat{q}_{1H0}=\hat{q}_{2H0}=0, \tag{C4}$$

$$\hat{q}_{1H1}=-\frac{5}{4}\hat{T}_{H0}\frac{d\hat{T}_{H0}}{dx_1},\quad \hat{q}_{2H1}=0, \tag{C5}$$

$$\hat{q}_{1H2}=-\frac{5}{4}\left(\hat{T}_{H0}\frac{d\hat{T}_{H1}}{dx_1}+\hat{T}_{H1}\frac{d\hat{T}_{H0}}{dx_1}\right), \tag{C6a}$$

$$\hat{q}_{2H2}=4\frac{\hat{T}_{H0}}{\hat{\rho}_{H0}}\frac{d\hat{T}_{H0}}{dx_1}\frac{d\hat{v}_{2H0}}{dx_1}+\frac{1}{2}\frac{\hat{T}_{H0}^2}{\hat{\rho}_{H0}}\frac{d^2\hat{v}_{2H0}}{dx_1^2}. \tag{C6b}$$

Note that $\hat{p}_{13Hm}=\hat{p}_{23Hm}=0$ and $\hat{q}_{3Hm}=0$.

APPENDIX D: KNUDSEN-LAYER PARTS OF THE MACROSCOPIC QUANTITIES

The expressions of h_{Km} in terms of $\hat{f}_{Km}$ for $\hat{\rho}_K$, $\hat{v}_{2K}$, $\hat{T}_K$, $\hat{p}_{ijK}$, and $\hat{q}_{iK}$ up to $m=2$ are summarized below. Here, the condition (34) has been used.

$$\hat{\rho}_{K1}=\int \hat{f}_{K1}d\boldsymbol{\zeta}, \tag{D1a}$$

$$\hat{v}_{2K1}=\frac{1}{(\hat{\rho}_{H0})_B}\int \zeta_2\hat{f}_{K1}d\boldsymbol{\zeta}, \tag{D1b}$$

$$\hat{T}_{K1}=\frac{2}{3(\hat{\rho}_{H0})_B}\int \left(\zeta^2-\frac{3}{2}\right)\hat{f}_{K1}d\boldsymbol{\zeta}, \tag{D1c}$$

$$\hat{p}_{11K1}=2\int \zeta_1^2\hat{f}_{K1}d\boldsymbol{\zeta}, \tag{D1d}$$

$$\hat{p}_{12K1}=2\int \zeta_1\zeta_2\hat{f}_{K1}d\boldsymbol{\zeta}, \tag{D1e}$$

$$\hat{p}_{22K1}=2\int \zeta_2^2\hat{f}_{K1}d\boldsymbol{\zeta}, \tag{D1f}$$

$$\hat{p}_{33K1}=2\int \zeta_3^2\hat{f}_{K1}d\boldsymbol{\zeta}, \tag{D1g}$$

$$\hat{q}_{1K1}=\int \zeta_1\zeta^2\hat{f}_{K1}d\boldsymbol{\zeta}, \tag{D1h}$$

$$\hat{q}_{2K1}=\int \zeta_2\zeta^2\hat{f}_{K1}d\boldsymbol{\zeta}-\tfrac{5}{2}(\hat{\rho}_{H0})_B\hat{v}_{2K1}, \tag{D1i}$$

$$\hat{\rho}_{K2}=\int \hat{f}_{K2}d\boldsymbol{\zeta}, \tag{D2a}$$

$$\hat{v}_{2K2}=\frac{1}{(\hat{\rho}_{H0})_B}\left\{\int \zeta_2\hat{f}_{K2}d\boldsymbol{\zeta}-\left[(\hat{\rho}_{H1})_B+\left(\frac{d\hat{\rho}_{H0}}{dy}\right)_B\eta\right]\hat{v}_{2K1} -\left[(\hat{v}_{2H1})_B+\left(\frac{d\hat{v}_{2H0}}{dy}\right)_B\eta\right]\hat{\rho}_{K1}-\hat{\rho}_{K1}\hat{v}_{2K1}\right\}, \tag{D2b}$$

$$\hat{T}_{K2}=\frac{1}{(\hat{\rho}_{H0})_B}\left\{\frac{2}{3}\int\left(\zeta^2-\frac{3}{2}\right)\hat{f}_{K2}d\boldsymbol{\zeta} -\left[(\hat{\rho}_{H1})_B+\left(\frac{d\hat{\rho}_{H0}}{dy}\right)_B\eta\right]\hat{T}_{K1} -\left[(\hat{T}_{H1})_B+\left(\frac{d\hat{T}_{H0}}{dy}\right)_B\eta\right]\hat{\rho}_{K1}-\hat{\rho}_{K1}\hat{T}_{K1}\right\} -\frac{4}{3}\left[(\hat{v}_{2H1})_B+\left(\frac{d\hat{v}_{2H0}}{dy}\right)_B\eta\right]\hat{v}_{2K1}-\frac{2}{3}\hat{v}_{2K1}^2, \tag{D2c}$$

$$\hat{p}_{11K2}=2\int \zeta_1^2\hat{f}_{K2}d\boldsymbol{\zeta}, \tag{D2d}$$

$$\hat{p}_{12K2}=2\int \zeta_1\zeta_2\hat{f}_{K2}d\boldsymbol{\zeta}, \tag{D2e}$$

$$\hat{p}_{22K2}=2\int \zeta_2^2\hat{f}_{K2}d\boldsymbol{\zeta}-2(\hat{\rho}_{H0})_B\hat{v}_{2K1}^2-4(\hat{\rho}_{H0})_B \times\left[(\hat{v}_{2H1})_B+\left(\frac{d\hat{v}_{2H0}}{dy}\right)_B\eta\right]\hat{v}_{2K1}, \tag{D2f}$$

$$\hat{p}_{33K2}=2\int \zeta_3^2\hat{f}_{K2}d\boldsymbol{\zeta}, \tag{D2g}$$

$$\hat{q}_{1K2}=\int \zeta_1\zeta^2\hat{f}_{K2}d\boldsymbol{\zeta}-(\hat{p}_{12H1})_B\hat{v}_{2K1} -\left[(\hat{v}_{2H1})_B+\left(\frac{d\hat{v}_{2H0}}{dy}\right)_B\eta+\hat{v}_{2K1}\right]\hat{p}_{12K1}, \tag{D2h}$$

$$\hat{q}_{2K2}=\int \zeta_2\zeta^2\hat{f}_{K2}d\zeta-\left[(\hat{v}_{2H1})_B+\left(\frac{d\hat{v}_{2H0}}{dy}\right)_B\eta+\hat{v}_{2K1}\right]\hat{p}_{22K1} -\frac{3}{2}[\hat{\rho}_{K1}+(\hat{\rho}_{H0})_B\hat{T}_{K1}]\left[(\hat{v}_{2H1})_B+\left(\frac{d\hat{v}_{2H0}}{dy}\right)_B\eta +\hat{v}_{2K1}\right]-\frac{5}{2}\left\{(\hat{\rho}_{H1})_B+\left(\frac{d\hat{\rho}_{H0}}{dy}\right)_B\eta+(\hat{\rho}_{H0})_B \times\left[(\hat{T}_{H1})_B+\left(\frac{d\hat{T}_{H0}}{dy}\right)_B\eta\right]\right\}\hat{v}_{2K1}-\frac{5}{2}(\hat{\rho}_{H0})_B\hat{v}_{2K2}, \tag{D2i}$$

where

$$\zeta^2=\zeta_y^2+\zeta_2^2+\zeta_3^2,\quad d\boldsymbol{\zeta}=d\zeta_y d\zeta_2 d\zeta_3, \tag{D3}$$

and $(\,)_B$ indicates the value on the wall ($y=0$). In addition to $\hat{p}_{13Km}=\hat{p}_{23Km}=0$ and $\hat{q}_{3Km}=0$, we have $\hat{p}_{11Km}=0$ because $\hat{p}_{11K}$ is given by $\hat{p}_{11K}=\hat{p}_{11}-\hat{p}_{11H}$, and $\hat{p}_{11}$ and $\hat{p}_{11H}$ are the same constant [note that Eq. (16a) holds also for $\hat{p}_{11H}$ because $\hat{f}_H$ is a solution of Eq. (9) and that $\hat{p}_{11}=\hat{p}_{11H}$ outside the Knudsen layer]. Furthermore, the relations $\hat{p}_{12K1}=\hat{p}_{12K2}=0$ and $\hat{q}_{1K1}=0$ hold. In fact, multiplying Eq. (47a) with $\zeta_2 E$ and $\zeta^2 E$, integrating with respect to ζ_i over its whole space, and taking into account the condition (47c), we have

$$\int \zeta_1\zeta_2\hat{f}_{Km}d\boldsymbol{\zeta}=\int \zeta_1\zeta^2\hat{f}_{Km}d\boldsymbol{\zeta}=0, \tag{D4}$$

for $m=1$ and 2, which, together with Eqs. (D1e), (D1h), and (D2e), leads to the relations mentioned above (note that $\hat{q}_{1K2}$ does not vanish).

[1] R. Esposito, J. L. Lebowitz, and R. Marra, Commun. Math. Phys. **160**, 49 (1994).
[2] M. Tij and A. Santos, J. Stat. Phys. **76**, 1399 (1994).
[3] M. Malek Mansour, F. Baras, and A. L. Garcia, Physica A **240**, 255 (1997).
[4] M. Tij, M. Sabbane, and A. Santos, Phys. Fluids **10**, 1021 (1998).
[5] D. Risso and P. Cordero, Phys. Rev. E **58**, 546 (1998).
[6] F. J. Uribe and A. L. Garcia, Phys. Rev. E **60**, 4063 (1999).
[7] S. Hess and M. Malek Mansour, Physica A **272**, 481 (1999).
[8] P. L. Bhatnagar, E. P. Gross, and M. Krook, Phys. Rev. **94**, 511 (1954).
[9] P. Welander, Ark. Fys. **7**, 507 (1954).
[10] M. N. Kogan, Appl. Math. Mech. **22**, 597 (1958).
[11] Y. Sone, in *Rarefied Gas Dynamics*, edited by L. Trilling and H. Y. Wachman (Academic, New York, 1969), p. 243.
[12] Y. Sone and K. Yamamoto, J. Phys. Soc. Jpn. **29**, 495 (1970); see also Y. Sone and Y. Onishi, *ibid.* **47**, 672 (1979).
[13] Y. Sone, in *Rarefied Gas Dynamics*, edited by D. Dini (Editrice Tecnico Scientifica, Pisa, Italy, 1971), Vol. 2, p. 737.
[14] Y. Sone, in *Advances in Kinetic Theory and Continuum Mechanics*, edited by R. Gatignol and Soubbaramayer (Springer, Berlin, 1991), p. 19.
[15] Y. Sone, K. Aoki, S. Takata, H. Sugimoto, and A. V. Bobylev, Phys. Fluids **8**, 628 (1996); *ibid.* **8**, 841(E) (1996).
[16] Y. Sone, C. Bardos, F. Golse, and H. Sugimoto, Eur. J. Mech. B/Fluids **19**, 325 (2000).
[17] Y. Sone and K. Aoki, *Molecular Gas Dynamics* (Asakura, Tokyo, 1994) (in Japanese).
[18] Y. Sone, *Theoretical and Numerical Analyses of the Boltzmann Equation—Theory and Analysis of Rarefied Gas Flows—, Lecture Notes* (Department of Aeronautics and Astronautics, Graduate School of Engineering, Kyoto University, 1998), Part I (http://www.users.kudpc.kyoto-u.ac.jp/~a50077/).
[19] Y. Sone, *Kinetic Theory and Fluid Dynamics*, Modeling and Simulation in Science, Engineering and Technology (Birkhäuser, Basel, in press).
[20] C. Cercignani, *Rarefied Gas Dynamics, From Basic Concepts to Actual Calculations* (Cambridge University Press, Cambridge, 2000).
[21] Y. Sone, H. Sugimoto, and K. Aoki, Phys. Fluids **11**, 476 (1999).
[22] H. Grad, in *Transport Theory*, edited by R. Bellman, G. Birkhoff, and I. Abu-Shumays (American Mathematical Society, Providence, 1969), p. 269.
[23] C. Bardos, R. E. Caflisch, and B. Nicolaenko, Commun. Pure Appl. Math. **39**, 323 (1986).
[24] C. Cercignani, in *Trends in Applications of Pure Mathematics to Mechanics*, edited by E. Kröner and K. Kirchgässner (Springer-Verlag, Berlin, 1986), p. 35.
[25] F. Golse and F. Poupaud, Math. Methods Appl. Sci. **11**, 483 (1989).
[26] Y. Sone, J. Phys. Soc. Jpn. **19**, 1463 (1964).
[27] Y. Sone, J. Phys. Soc. Jpn. **20**, 222 (1965).
[28] Y. Sone and Y. Onishi, J. Phys. Soc. Jpn. **35**, 1773 (1973).
[29] Y. Sone and Y. Onishi, J. Phys. Soc. Jpn. **44**, 1981 (1978).
[30] T. Ohwada, Y. Sone, and K. Aoki, Phys. Fluids A **1**, 1588 (1989).
[31] Y. Sone, T. Ohwada, and K. Aoki, Phys. Fluids A **1**, 363 (1989).
[32] S. Chapman and T. G. Cowling, *The Mathematical Theory of Non-Uniform Gases*, 3rd ed. (Cambridge University Press, London, 1970), Chap. 15.
[33] T. Ohwada, Y. Sone, and K. Aoki, Phys. Fluids A **1**, 2042 (1989).
[34] M. Tij and A. Santos, Physica A **289**, 336 (2001).
[35] C. K. Chu, Phys. Fluids **8**, 12 (1965).
[36] K. Aoki, K. Nishino, Y. Sone, and H. Sugimoto, Phys. Fluids A **3**, 2260 (1991).
[37] Y. Sone, T. Ohwada, and K. Aoki, Phys. Fluids A **1**, 1398 (1989).
[38] M. Knudsen, *The Kinetic Theory of Gases*, 3rd ed. (Methuen, London, 1950).
[39] E. H. Kennard, *Kinetic Theory of Gases* (McGraw-Hill, New York, 1938).
[40] Y. Sone, J. Phys. Soc. Jpn. **21**, 1836 (1966).
[41] Y. Sone, K. Sawada, and H. Hirano, Eur. J. Mech. B/Fluids **13**, 299 (1994).
[42] V. S. Galkin, M. N. Kogan, and O. G. Fridlender, Mekh. Zhid. Gaza **3**, 98 (1971) [Fluid Dyn. **6**, 448 (1971)].
[43] M. N. Kogan, V. S. Galkin, and O. G. Fridlender, Usp. Fiz. Nauk. **119**, 111 (1976) [Sov. Phys. Usp. **19**, 420 (1976)].
[44] Y. Sone, S. Takata, and H. Sugimoto, Phys. Fluids **8**, 3403 (1996); *ibid.* **10**, 1239(E) (1998).
[45] Y. Sone, in *Rarefied Gas Dynamics*, edited by C. Shen (Peking University Press, Beijing, 1997), p. 3.
[46] Y. Sone, in *Annual Review of Fluid Mechanics* (Annual Reviews, Palo Alto, 2000), Vol. 32, p. 779.
[47] F. Bouchut, F. Golse, and M. Pulvirenti, *Kinetic Equations and Asymptotic Theory*, edited by B. Perthame and L. Desvillettes (Gauthier-Villars, Paris, 2000), Chap. 2.